Research on drone and urban air mobility noise

Measurement, modelling, and human perception

Snellen, M.; Merino Martinez, R.; Altena, A.; Amiri Simkooei, A.; Andino Cappagli, C.I.; Morin, A.M.; Yunus, F.; Yupa Villanueva, R.M.

Publication date
2024

Document Version
Final published version

Published in
QUIETDRONES 2024

QUIETDRONES 2024
MANCHESTER
8th - 11th September 2024

Research on drone and urban air mobility noise: Measurement, modelling, and human perception

Session: Keynote session

Mirjam Snellen and Roberto Merino-Martinez, Delft University of Technology, the Netherlands, Shared first coauthorship
m.snellen@tudelft.nl and r.merinomartinez@tudelft.nl
Anique Altena, Delft University of Technology, the Netherlands
a.altena@tudelft.nl
Alireza Amiri-Simkooei, Delft University of Technology, the Netherlands
a.amirisimkooei@tudelft.nl
Camilo I. Andino Cappagli, Delft University of Technology, the Netherlands
c.i.andinocappagli@tudelft.nl
Amy Morin, Delft University of Technology, the Netherlands a.m.morin@tudelft.nl
Luca N. Quaroni, Delft University of Technology, the Netherlands
l.n.quaroni@tudelft.nl
Furkat Yunus, Delft University of Technology, the Netherlands f.yunus@tudelft.nl
Renatto M. Yupa-Villanueva, Delft University of Technology, the Netherlands
r.m.yupavillanueva@tudelft.nl

Abstract This manuscript summarizes the main recent research efforts at Delft University of Technology in the field of drone and urban air mobility (UAM) vehicle noise. Illustrative examples are showcased, specifically in terms of acoustic measurements (both in-field and in wind-tunnel facilities), noise modelling (both data-driven and physics-based), and human perception of these sounds. In particular, the measurements feature microphone arrays and acoustic imaging to detect, localize, and isolate drone noise emissions. Regarding drone noise modelling, the proposed approaches cover noise generation, propagation, and acoustic footprint calculation. The evaluation of the human perception of drone noise and the perceived annoyance is another crucial aspect. To this end, psychoacoustic listening experiments are conducted in laboratory conditions and the results are analyzed using perception-based sound metrics. Data from aeroacoustic measurements and synthetic sound auralizations are considered. Combining these three main approaches holistically, the perception-driven design and assessment can be performed by targeting the minimization of the perceived noise annoyance, rather than merely reducing sound pressure levels.

Keywords: Drone noise; Psychoacoustics; Listening Experiments; Flyover Measurements.

1. Introduction

Whereas the expanding utilization of drones (also referred to as unmanned aerial vehicles, UAVs) presents promising opportunities (e.g. aerial photography, delivery services, emergency assessment, environmental monitoring, etc.), it simultaneously raises substantial concerns with respect to noise pollution. In addition, Urban Air Mobility (UAM) vehicles are currently not widely used yet, but future forecasts suggest that they will be soaring our skies in the near future. The development of models for predicting the noise of drones is an active field of research (Dreier & Vorländer, 2024). A number of complementary approaches exist, ranging from detailed physics-based prediction models to fully empirical models. In this contribution, these various approaches are addressed while highlighting the important potential contribution of outdoor measurements in the model development and validation. These allow for the noise assessment for a wide range of drone types and maneuvers. To minimize contributions from other sound sources and propagation effects, such as ground reflections, the use of acoustic arrays for taking these measurements is strongly recommended.

Typical drone sounds present different acoustic aspects compared to other familiar sources of environmental noise, such as road traffic (Bazilinskyy, Merino-Martinez, Özcan, Dodou, & de Winter, n.d.), aircraft (Merino-Martinez, Heblij, Bergmans, Snellen, & Simons, 2019), or wind turbines (Merino-Martinez, Pieren, & Schäffer, 2021). In fact, despite emitting typically lower sound levels than other sources, the high-frequency and tonal content of their noise signatures and their relatively closer proximity to the population could likely raise potential concerns about their social acceptance (Gwak, Han, & Lee, 2020; Yupa-Villanueva, Merino-Martinez, Altena, & Snellen, 2024). Some recent literature even suggests that for the same noise exposure (expressed as equivalent A-weighted sound pressure level, $L_{p,A,eq}$), drones are perceived as considerably more annoying than commercial aircraft (Gwak et al., 2020). Therefore, the noise emissions of these devices have attracted increasing interest from the industrial and scientific communities (Rizzi et al., 2020; Schäffer, Pieren, Heutschi, Wunderli, & Becker, 2021; Green, Torija, & Ramos-Romero, 2024).

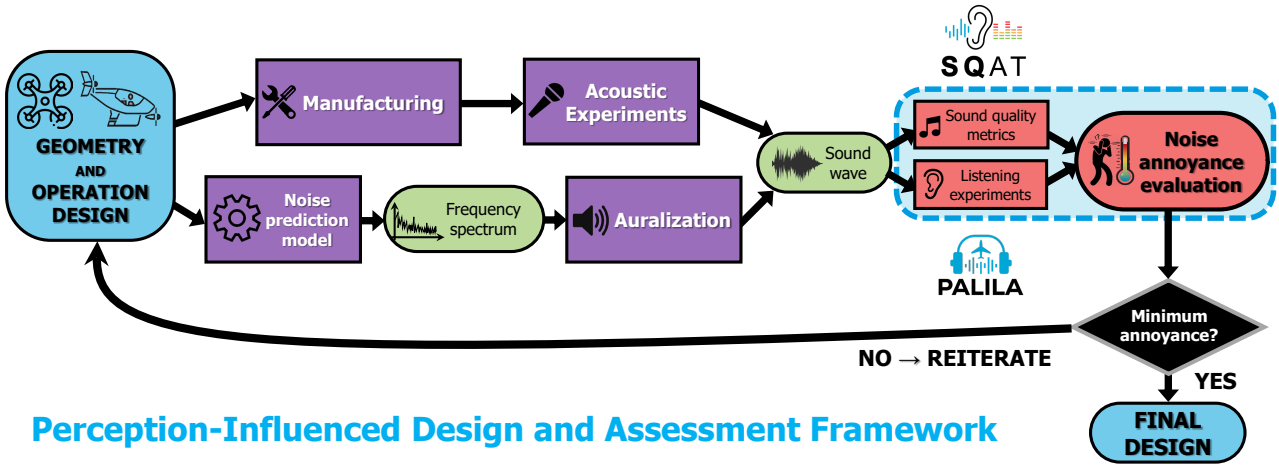

Figure 1: Overview of the proposed perception-influenced design and assessment framework for drones and UAM vehicles.

The current paper provides a general (non-exhaustive) overview of the research efforts recently conducted at Delft University of Technology (TU Delft) in the Netherlands focused on drone and UAM vehicle noise. These investigations can be conveyed in a holistic manner in a perception-influenced design and assessment framework, see Fig. 1. This framework can be divided into three main pillars:

1. **Acoustic measurements** (section 2), including full-scale field experiments (section 2.1) and measurements in laboratory conditions (section 2.2). This approach provides

essential information on the acoustic signature of the device or component under evaluation, provided that a physical model already exists. In particular, the measurement examples presented here make use of microphone arrays (see Fig. 2) and acoustic imaging methods (Merino-Martinez, Sijtsma, et al., 2019) to detect, localize, and isolate drone noise emissions from the ambient sounds and reflections, see Fig. 3.

2. **Noise modelling** (section 3), including data-driven (section 3.1) and physics-based (3.2) methods. These techniques are useful for assessing the noise emissions of designs or procedures that may not exist in reality yet. Most models provide information in the frequency domain that is not audible. Therefore, auralization techniques (Vorländer, 2008; Thoma, Merino-Martinez, Grönstedt, & Zhao, 2024; Dreier & Vorländer, 2024) (the acoustical counterpart of visualization) are typically employed to convert these predictions into audio files.

3. **Human perception** (section 4) of the sound signatures of drones and UAM vehicles is a critical aspect for ensuring their societal acceptance. The psychoacoustic perception of these sounds can be evaluated using state-of-the-art sound quality metrics (Greco, Merino-Martinez, Osses, & Langer, 2023) and listening experiments (Merino-Martinez, von den Hoff, & Simons, 2023). The latter approach is preferred, but it is normally unfeasible to evaluate all the (typically large number of) iterations within usual design processes.

Since drones and UAM are not as prevalent as other sources of environmental noise (e.g. aircraft, road traffic), the present moment represents a unique opportunity to draw lessons from past shortcomings in noise assessment and sound design. This allows for the development of low-annoyance devices that can be harmoniously integrated into current soundscapes, minimizing disturbances to the living environment.

This paper summarizes the content presented by the first two authors in a keynote lecture during this conference.

2. ACOUSTIC MEASUREMENTS

2.1 Full-scale field experiments

Given the large variety of drone configurations and operations, outdoor measurements are a crucial element in the realization of empirical noise models for predicting drone noise and evaluating its annoyance. To develop such assessment tools and models, a broad and comprehensive database of drone noise in outdoor areas, reflective of realistic conditions, is required. In such studies, the acoustic measurements have to be recorded in conjunction with several drone telemetry records to characterize operational conditions. Such operations also need to be comprehensive in terms of all the maneuvers that characterize a typical flight envelope. In addition, they have to be representative of different flight dynamics variables, such as drone velocity and mass, and they have to be repetitive; several replicates need to be recorded to assess and quantify variability in a -mostly- non-controlled environment.

Outdoor experiments, although informative and irreplaceable, have an inherent variability caused by factors, such as environmental conditions, like wind gusts, and the presence of other sound sources in the local airspace (Ramos-Romero, Green, Torija, & Asensio, 2023). Therefore, the use of microphone arrays (see Fig. 2) is highly preferable.

These devices are beneficial compared to single microphone systems for two reasons:

First, the signal-to-noise ratio can be significantly improved compared to single-microphone measurements by focusing the array in the desired direction through beamforming techniques (Merino-Martinez, 2024). From the resulting microphone array measurements, high-

quality databases can be created and used to develop noise prediction models for drone operations.

Secondly, the microphone array's localization capabilities can be used to synchronize data from different sources, such as the GPS measurements of the drone. In addition, the measurement geometry (relative array location and orientation) can be estimated by maximizing the match between acoustic localizations and those of the GPS, for example. It should be noted that due to the rapid increase in the use and availability of drones, the development of acoustic localization techniques is, in addition to the application mentioned above, an important research topic. The reason is that drones might pose a threat to public safety, both intentionally and unintentionally. To mitigate this threat, drones must be located in a timely manner. Acoustic localization techniques can serve as a solution for this, see Fig. 3. The benefits of acoustic localization techniques, compared to other techniques, are the relatively low costs and the passive behavior.

Figure 2: Examples of the microphone arrays employed in field measurements. (a) 64-microphone array (PUI Audio 665-POM-2735P-R) distributed in a multi-arm spiral configuration. (b) CAE Bionic M-112 microphone array measuring the noise emissions of a hovering drone.

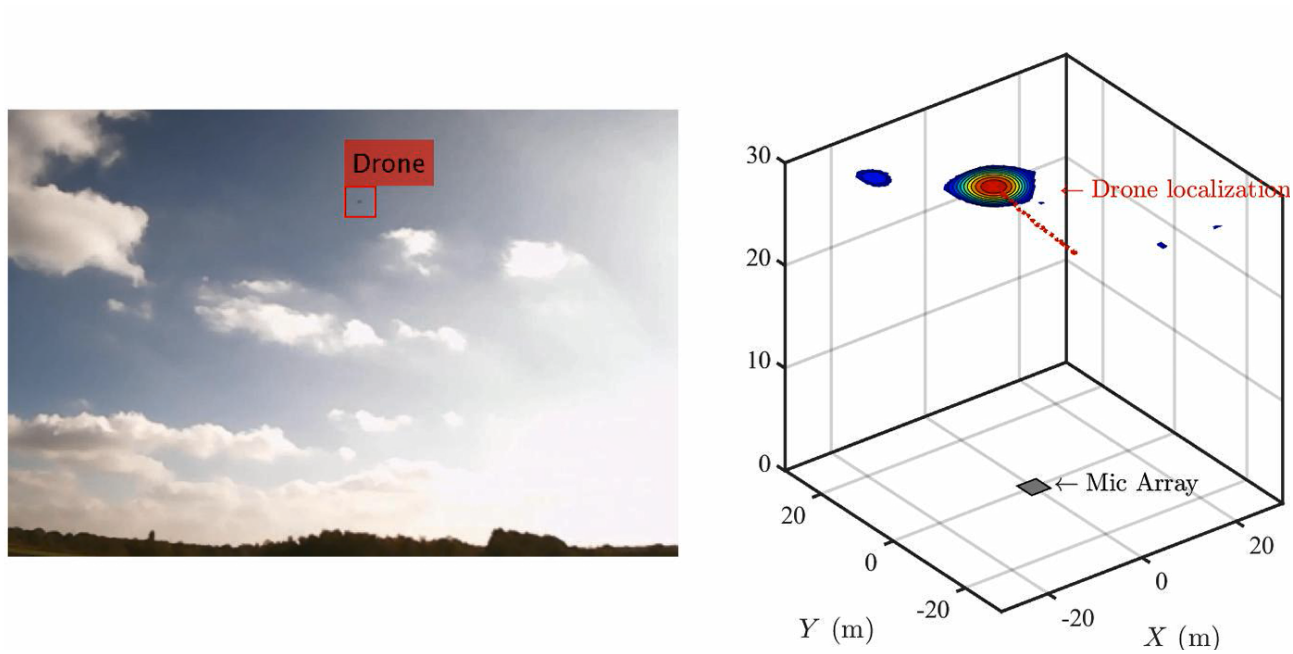

Figure 3: Drone detection and localization using frequency-domain acoustic beamforming supported by optical camera measurements. This plot is an animated version of the results of (Altena et al., 2023)

2.2 Measurements in laboratory facilities

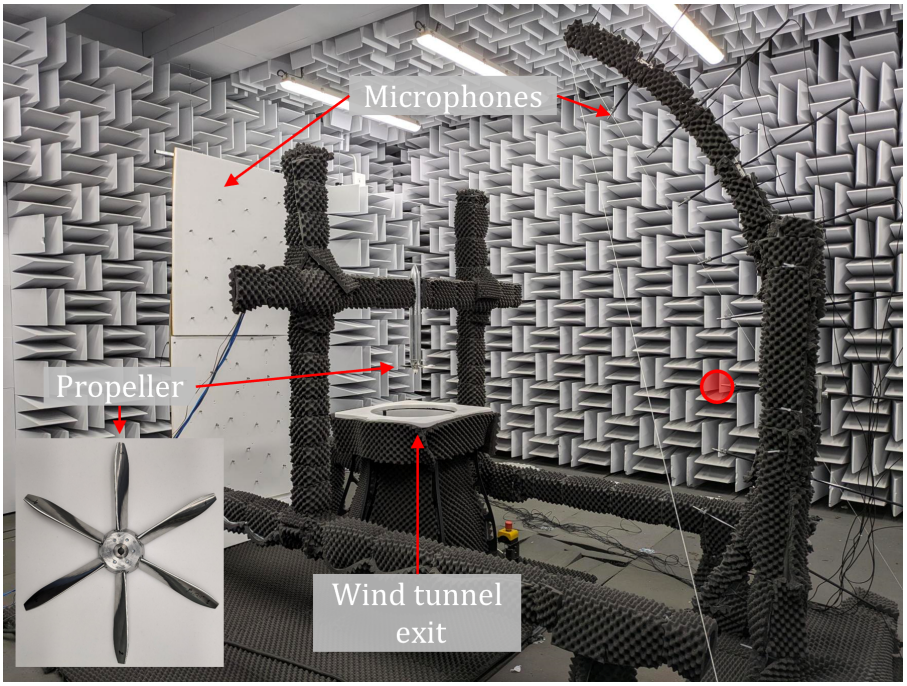

Figure 4: Experimental setup at the anechoic 'A-Tunnel' open-jet facility of TU Delft for the aeroacoustic analysis of propeller turbulence ingestion noise. The red circle denotes the microphone position for the data reported in Figure 5.

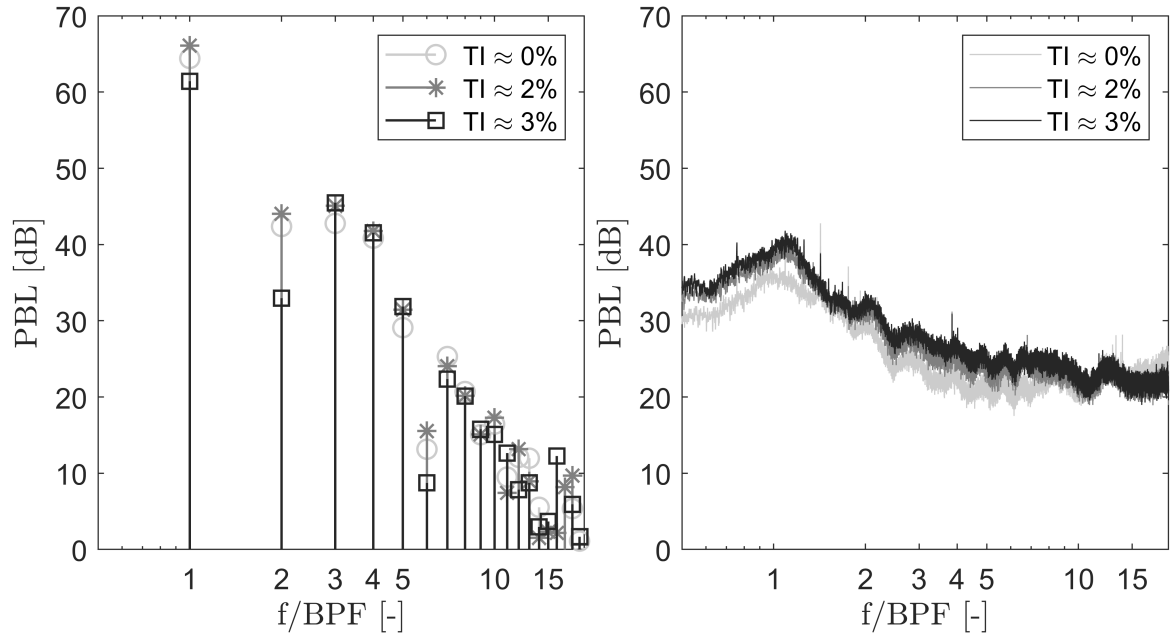

Figure 5: Pressure Band Level (PBL, $df = 0.84$ Hz and $p_{ref} = 20$ μPa) of the acoustic pressure measured at the propeller plane (at a distance of 1.3 m from the rotational axis) for different inflow turbulence intensity (TI) levels and constant inflow velocity of 25 m/s and Blade Passing Frequency (BPF) of 1012.6 Hz. Left: tonal component at BPF harmonics, right: broadband component.

Testing in laboratory facilities allows for greater control over the operating flow conditions and environmental factors than what is possible during field measurements. This, in turn, permits a more detailed parametric investigation of the effects of specific parameters (e.g. number of blades, incoming turbulence) on the phenomenon under consideration. Laboratory measurement campaigns are therefore particularly well-suited for fundamental studies

aimed at providing reliable data for the validation of theoretical and numerical models (Allen et al., 2002).

Anechoic chambers are typically employed for the acoustic characterization of drones or propellers in static hover conditions, e.g. (Tinney & Sirohi, 2018; Heutschi, Ott, Nussbaumer, & Wellig, 2020; Merino-Martinez, Ben-Gida, & Snellen, 2024). Low-speed, open-jet wind tunnels with anechoic plenums are instead used in the study of propellers subject to differing types of inflow conditions, e.g. (Petricelli et al., 2023). The anechoic 'A-Tunnel' facility at TU Delft belongs to the latter type; a comprehensive description of it can be found in (Merino-Martínez et al., 2020). Propeller noise has been the subject of a number of experimental campaigns in this facility, with the aim to provide more insights into the noise generation mechanisms of low-Reynolds number propellers present in drones (Casalino, Grande, Romani, Ragni, & Avallone, 2021; Grande, Romani, Ragni, Avallone, & Casalino, 2022; Baars & Ragni, 2024).

The recent rise in Unmanned Aerial Vehicles (UAVs) and novel aircraft propulsion technologies involving the use of rotors (e.g. boundary layer ingestion (BLI), distributed electric systems) has led to a renewed interest in propeller aeroacoustics. Within this context, the influence of nearly-isotropic grid-generated turbulence ingestion by an isolated propeller on the far-field noise emissions has recently been investigated at the 'A-Tunnel' facility. Preliminary results of these campaigns can be found in (Piccolo, Zamponi, Avallone, & Ragni, 2024; Quaroni, Merino-Martinez, Monteiro, & Kumar, 2024). The latter study in particular focused on the effects of the characteristics of the inflow turbulence (i.e. turbulence intensity TI and streamwise integral lengthscale Λ_x) on the noise emissions of a six-bladed propeller model (referred to as X-PROP-S) with a radius of 101.6 mm and adjustable blade pitch angle β. The geometry of the propeller, as well as its aerodynamic characteristics, can be found in (Van Arnhem et al., 2020). Figure 4 depicts a picture of the experimental setup employed, featuring two microphone arrays: a 64-microphone planar one (on the left) and an 8-microphone directivity arc (on the right). Figure 5 shows the influence of the incoming turbulence characteristics on both the tonal and broadband components of the noise emissions recorded at a distance of 1.3 m from the rotor's shaft and in the propeller plane (see red circle in Fig. 4). The results for three different TI values are reported: 0%, 2%, and 3%. In general, the broadband noise emissions increase with the increasing TI values. Interestingly, the noise levels of the first two tones and some of the higher harmonics are attenuated to some extent when the TI is increased. Ongoing further analyses are possible by considering data from both microphone arrays and aerodynamic measurements (hot-wire anemometry for incoming turbulence spectral characterization and traversing pressure probes for blade loading estimation, see (Quaroni et al., 2024)).

The same propeller geometry shown in Fig. 4 (X-PROP-S) was also tested in a distributed-propulsion configuration, see Fig. 6(a) featuring three identical six-bladed steel propellers (Monteiro, Merino-Martinez, & Lima Pereira, 2024). This configuration is representative of multi-propeller configurations in unconventional aircraft configurations and several UAM vehicle designs (Schade et al., 2024). The three propellers were tested in the closed-section low-turbulence wind tunnel (LTT) of TU Delft and placed approximately 85 mm away from the leading edge of a wing angled 5° downward relative to the wing chord. A tip clearance of 4.8 mm between adjacent propellers was set. This experimental setup enables setting the relative blade phase angle $\Delta\phi$ between adjacent propellers under synchrophasing conditions with a precision of 0.16° standard deviation, to investigate its influence on the generated noise emissions. A planar 64-microphone array was placed behind a Kevlar window to prevent the turbulent boundary layer of the wind tunnel wall from contaminating the recorded acoustic signals (Bento et al., 2023). For further details on the experimental setup, the interested reader is referred to (Monteiro et al., 2024).

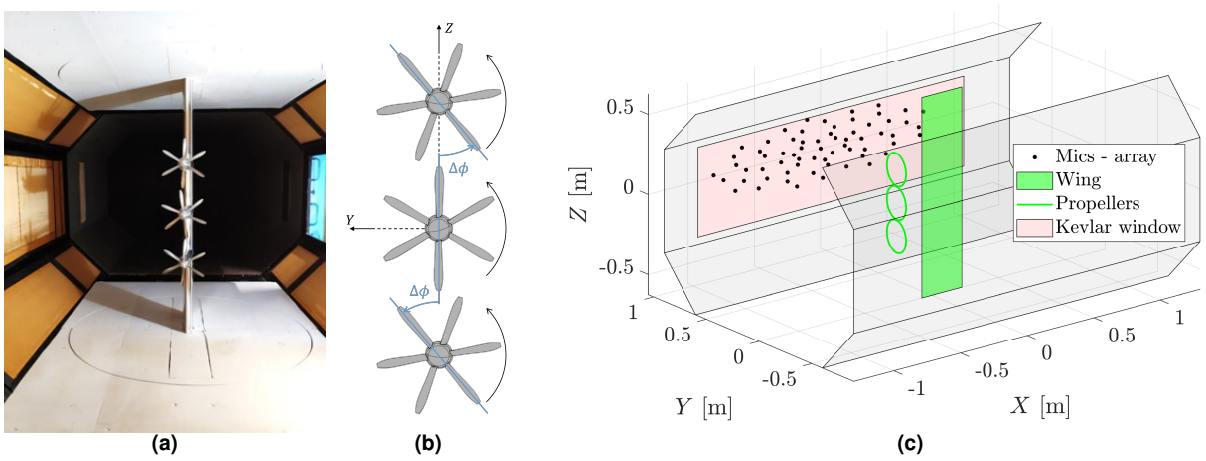

Figure 6: (a) Experimental setup inside the acoustic test section of the low-turbulence wind tunnel (LTT) of TU Delft. (b) Definition of relative blade-phase angle $\Delta\phi$. (c) Microphone array positioning behind the Kevlar window. Adapted from (Monteiro et al., 2024).

A total of six different relative blade-phase angles $\Delta\phi$ were considered: $0°$, $10°$, $20°$, $30°$, $40°$, and $50°$, as well as a baseline case with random $\Delta\phi$ values. The results presented here refer to three different microphones located approximately at emission angles θ of $52°$ (upstream direction), $90°$ (flyover direction), and $125°$ (downstream direction). A freestream velocity of 30 m/s and a wing angle of attack of $2°$ were considered. These conditions correspond to a blade tip Mach number of 0.35, and Reynolds numbers at the tip of approximately 6.0×10^4.

Figure 7 depicts the noise emissions in the three selected microphones for the different $\Delta\phi$ values. Two different sound metrics are considered: the maximum A-weighted sound pressure level ($L_{\text{p,A,max}}$) and the maximum tone-corrected perceived noise level (PNLT_{max}) (Merino-Martinez, 2018). The PNLT includes a tone penalty based on the one-third-octave band spectrum, which is an adjustment for sounds with noticeable tonal components. The highest noise emissions are observed in all cases for $\Delta\phi = 0°$, whereas the cases of $\Delta\phi = 20°$ and $\Delta\phi = 30°$ present considerable noise reductions (up to 10 dBA and 8 PNLTdB), especially in the downstream direction. The original reference (Monteiro et al., 2024) contains the results corresponding to more sound metrics (including psychoacoustic indicators) and operational conditions. These preliminary results indicate the potential of synchrophasing in distributed propulsion systems for noise reduction.

3. Noise Modelling

Noise prediction models are essential tools to predict the acoustic signature of drones and UAM vehicles, which enable the assessment of different configurations and operational conditions and their corresponding perceptual impact on the ground. Therefore, these methods are crucial for devising noise mitigation strategies.

When modelling drone noise, two common approaches, namely empirical or data-driven methods and physics-based (PB) methods, can be used. The models should link the sound metrics to the operational parameters of the drone, such as position, velocity, and blade passing frequency (BPF). Each type of method has its own strengths and limitations. A brief review of these is provided below.

Empirical data-driven methods leverage data collected from acoustic measurements to create predictive models for drone and UAM vehicle noise. By applying machine learning (ML) methods to these measurements relationships between input variables (e.g. position, velocity, BPF) and sound metrics can be established without modelling the physics explic-

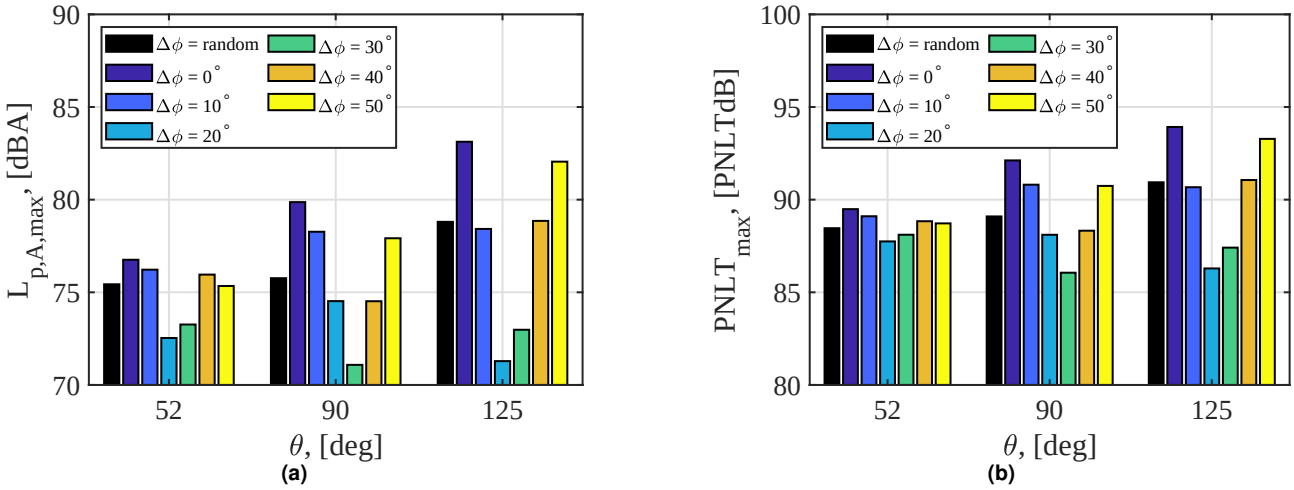

Figure 7: Noise emissions as a function of the relative blade phase angle $\Delta\phi$ at $\theta = 52°$, $90°$ and $125°$: (a) $L_{p,A,max}$, (b) $PNLT_{max}$

itly. The advantages of ML methods are that, once trained, they can provide near-real-time predictions of noise levels based on input parameters, which makes them highly efficient for real-time applications. ML models can also easily incorporate different operational parameters and environmental factors, such as wind speed, altitude, and atmospheric conditions into the noise prediction model without needing complex mathematical formulations. When trained on large datasets, data-driven models can, in principle, generalize across different drones and operating environments. This is valuable for assessing a wide range of scenarios without needing detailed and drone-specific physical models. On the other hand, there are also drawbacks to ML methods. The performance of ML models is heavily dependent on the quality and quantity of the training data, which can be a challenging problem. When modelling the noise performance over a typical set of maneuvers using ML, it is necessary to have experimental data representative of such maneuvers from which the model can generalize for similar operations. In addition, unlike PB models, empirical methods lack direct ties to physical laws, which can make it difficult to understand the (variations in) predicted noise metrics.

Physics-based methods rely on fundamental physical principles to model sound generation, propagation, and interactions with the environment. In recent years, both high-fidelity and low-order PB methods have been widely used to study drone noise generation and propagation in urban environments. Whereas high-fidelity methods offer detailed insights, they become computationally impractical for larger propagation distances, higher frequencies, and varying outdoor operating conditions. Consequently, the main drone noise PB prediction approach at TU Delft emphasizes low-order methods, which are specifically developed to handle these practical challenges.

3.1 Data-driven models

In general, the data-driven methodology to predict the noise from drone operations researched at TU Delft focuses on understanding empirical relations between operational conditions and the noise signatures of different UAV types. For this, variables representative of operational conditions are defined as features in the frame of ML and statistical modelling approaches. Since the ultimate goal is to prescribe the noise annoyance at observer points, sound metrics are defined as the output variables whose dynamics have to be predicted.

Initial efforts in this area focused on exploring potential linear relationships that could link operational parameters with acoustic metrics. For this, several acoustic metrics were extracted from data obtained in experimental field campaigns, which represent distinct acoustic

features. These were the overall sound pressure level (OSPL, separated as both broadband and tonal), the acoustic power dispersion of the tones (as a measure of how heterogeneous the tonal energy is), and the number of tones present as a function of time (also as a measure of heterogeneity but in the frequency domain). In this way, these observables build parameters of the tonal sound pressure level distribution as a function of time. To build the feature matrix, GPS data recorded during the corresponding experimental campaigns were used; relative positions, velocities, and accelerations were computed as features. To study the adequacy of linear models, an electric vertical take-off and landing (eVTOL) drone fixed wing, see Fig. 8, operated by the company ANWB was studied during flybys over or next to the microphone array. The drone takes off and lands vertically as a quadcopter, using the 4 vertical rotors. For forward flight maneuvers, the horizontal propeller is used while the 4 rotors only operate in case additional trajectory stabilization and maneuverability are required.

Figure 8: Photo from the eVTOL Avy Aera 3.

Formally, the acoustic metric of interest is allocated to an output vector y, with the number of components corresponding to each realization of the quantity in time, while each operational parameter vector a becomes a column in a feature matrix A, such that the number of columns corresponds to the number of operational parameters considered, and the number of rows to the number of realizations or data points. Assuming a linear relation between these two groups of variables means that there is a scalar x_i that connects the operational parameter a_i (i^{th} column of A) and the acoustic observable or output y. In matrix notation, this relationship can be represented as $y = Ax + e$, where each entry of x corresponds to the scalar x_i associated with the i^{th} operational parameter. The vector e represents the residual vector, indicating the deviation from the linear assumption. Furthermore, to keep the assumptions simple, the parameters x are estimated using the least-squares theory; therefore the estimated value of x is $\hat{x} = (A^T Q_y^{-1} A)^{-1} A^T Q_y^{-1} y$, with Q_y the dispersion matrix (covariance matrix) of the observations. This estimation allows to compute an estimated value of y, $\hat{y} = A\hat{x}$, and also an estimate for the error $\hat{e} = y - \hat{y}$.

By splitting the pertinent data into a training set, from which x is calculated, and a validation set, it is possible to assess the performance of the approach and the best linear model. In these scenarios, the training performance can be evaluated using the test statistics $T_q = \hat{e}^T Q_y^{-1} \hat{e}$ and assessing whether it is smaller than a certain critical value (Teunissen, 2000). The linear model presented here was determined by finding the combination of operational parameters for which the resultant model gave the smallest test statistic $T_q = \hat{e}^T Q_y^{-1} \hat{e}$.

In Figure 9, some results corresponding to the OSPL analysis can be observed. It was found that in most cases, the overall time-dependent behavior is recovered, both at the training (Fig. 9(a)) and prediction (Fig. 9(b)) cases. In Fig. 9(a), the linear model parameters were trained, where the model manages to reconstruct the trend of the signal, but not the

detailed variations. This behavior is also observed in the validation results from Fig. 9(b). For some instances, it is observed that the model does not manage to trace sudden changes in OSPL, which can be seen around the secondary crests of the different signals.

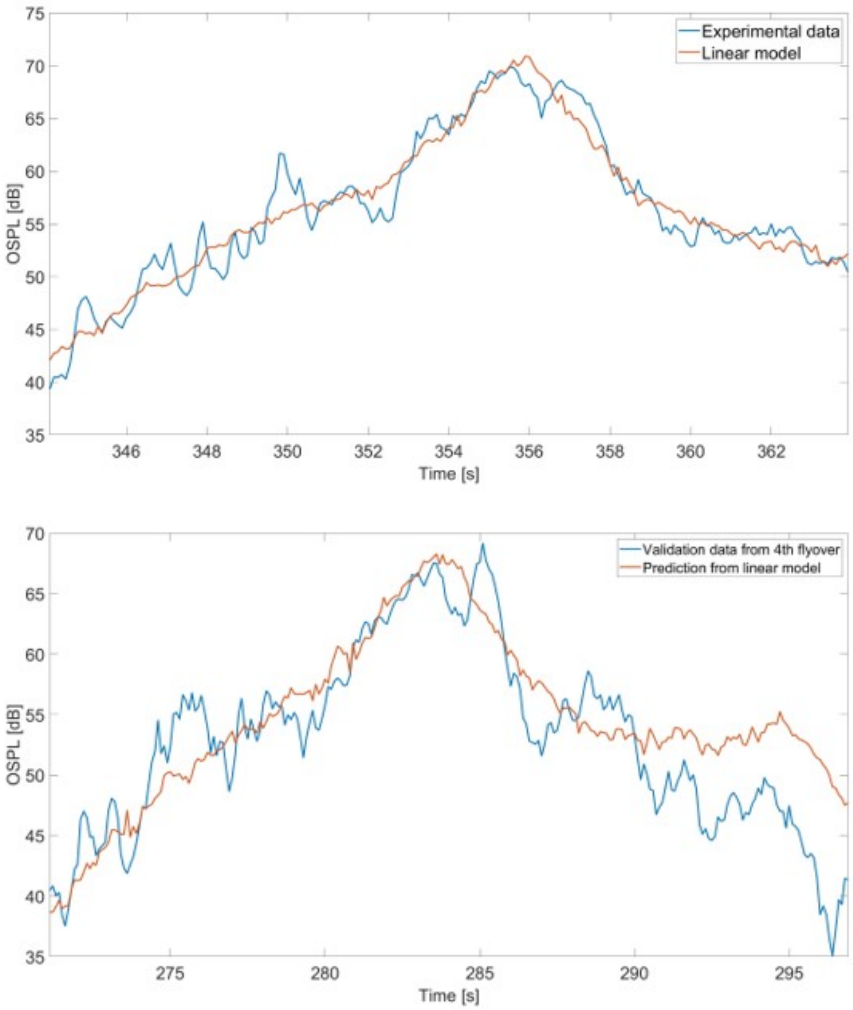

Figure 9: Example of the linear data-driven OSPL prediction model for the Avy Aera 3 drone for training and validation cases.

Given the results and the underlying assumptions, this approach has limitations and should serve as a preliminary guide to develop more sophisticated and accurate models. The current assumption that a linear relationship exists between operational parameters and acoustic metrics is too simplistic. Also, the available telemetry data is insufficient, as rotor-specific information was not included in the current study. Nonetheless, this approach did capture the general trends, which will need to be represented, either directly or indirectly, in more advanced models moving forward.

Predicting drone noise from operational parameters can also be performed through various machine learning (ML) methods, including support vector regression (SVR), random forest (RF), multilayer perceptron (MLP), and a recently developed method called least-squares-based deep learning (LSBDL). As feature-based ML methods, they offer unique advantages for drone noise prediction. They can be used to capture complex and non-linear relationships between input features and the resulting noise at observer locations. SVR maps input data to a high-dimensional feature space (Awad & Khanna, 2015), where it seeks to model intricate patterns in the operational conditions and acoustic metrics. This can be effective in capturing subtle variations in noise levels that simple linear models may overlook. RF is a robust ensemble-learning technique that combines the outputs of numer-

ous decision trees (Breiman, 2001; Sabzehee, Amiri-Simkooei, Iran-Pour, Vishwakarma, & Kerachian, 2023), offering resilience to noise in the data and the ability to model complex interactions without overfitting. In drone noise studies, RF can be applied to predict acoustic metrics by analyzing how variables such as GPS-derived velocities or positions correlate with overall sound pressure levels (OSPL) and tonal noise components. RF's ensemble approach averages the predictions of individual trees, enhancing reliability in varying operational conditions. MLP, as a fully connected feed-forward neural network, is also used to approximate nonlinear relationships (Ezugwu, Fadare, Bonney, Da Silva, & Sales, 2005). With sufficient training data, MLP can also effectively learn to represent the relationships between flight parameters and noise levels.

As an innovative approach, LSBDL combines the principles of least-squares estimation with deep learning techniques (Amiri-Simkooei, Tiberius, & Lindenbergh, 2024). This method establishes the linear relationship $y = Ax + e$ by using a feature matrix D in the following form:

$$y = Ax + e = \mathtt{A}(DW)x + e, \tag{1}$$

where $\mathtt{A}(.)$ represents an activation function, and W denotes the trainable weights and biases, to be optimized, for example, through a gradient descent method. In conjunction with the explainable artificial intelligence (XAI), LSBDL offers three important benefits for drone noise prediction: 1) LSBDL allows the direct calculation of the covariance matrix for the predicted outcomes, which is valuable in assessing the uncertainty in predictions of drone noise levels. 2) LSBDL provides a basis for hypothesis testing and outlier detection, which is essential when sound metrics are derived from real-world drone operations. By flagging outliers, LSBDL improves model robustness, making it better suited to capture and predict fluctuating noise patterns in various operational settings. 3) Drone noise datasets are often diverse due to different operational conditions. LSBDL uses the covariance matrix of training data to handle inconsistent, heterogeneous, and statistically correlated data, making it a practical choice for real-world applications.

3.2 Physics-based model

The current physics-based approach in TU Delft for predicting drone noise is mainly focused on predicting propeller noise under different operating conditions. Propeller noise spectra are characterized by the presence of both tonal and broadband components.

Tonal noise arises from deterministic sources, including thickness noise, which is due to the fluid displaced by the moving blades, steady-loading noise, which is caused by the steady forces acting on the blades, and unsteady-loading noise, which primarily results from local distortions in the inflow or non-axial inflow conditions, e.g. when the propeller shaft is not aligned with the incoming airflow. In non-axial inflow, each blade experiences periodic variations in the local angle of attack, leading to fluctuations in blade loading that generate periodic unsteady-loading noise at harmonics of the blade-passage frequency (BPF) (Magliozzi, Hanson, & Amiet, 1991). This situation commonly occurs during conversion flight and forward flight conditions of drones and UAM vehicles with significant variation in radiation and directivity of the noise compared to hovering conditions. The current noise prediction approach accounts for all aforementioned tonal noise mechanisms in drone noise prediction.

Broadband noise, on the other hand, includes turbulence ingestion noise, blade-wake interaction noise, and blade self-noise. The latter originates from fluctuations in the boundary layer or from separations and vortex shedding. This is the only broadband noise generation mechanism considered in the current noise prediction approach.

Although high-fidelity computational fluid dynamics (CFD) methods are commonly used to study propeller noise, the current prediction approach relies primarily on low-order methods to enable their use in impact assessment and optimization studies. These methods are

computationally efficient and still provide reliable results. Low-order approaches predict propeller noise by coupling aerodynamic and acoustic models. Among the most widely used aerodynamic models is the blade element momentum theory (BEMT), which offers accuracy comparable to CFD but with significantly reduced computational cost. In the in-house low-order propeller noise prediction solver (LOPNOR), BEMT is employed to calculate the aerodynamic forces that contribute to both steady and unsteady loading noise, especially under non-axial inflow conditions.

Two different frequency domain aeroacoustic formulations are implemented in LOPNOR. The first one is based on the later work of Hanson that accounts for the effects of non-compactness, sweep, and non-axial flow (1D) (Hanson, 1990). Our recent work (Yunus, von den Hoff, & Snellen, 2024) has demonstrated that LOPNOR predictions with the Hanson formulation showed very satisfactory agreement with a high-fidelity simulation and several outdoor measurements from multiple aircraft flyover events. A direct comparison of time-level histories of several flyovers between LOPNOR predictions and outdoor measurements is depicted in Fig. 10.

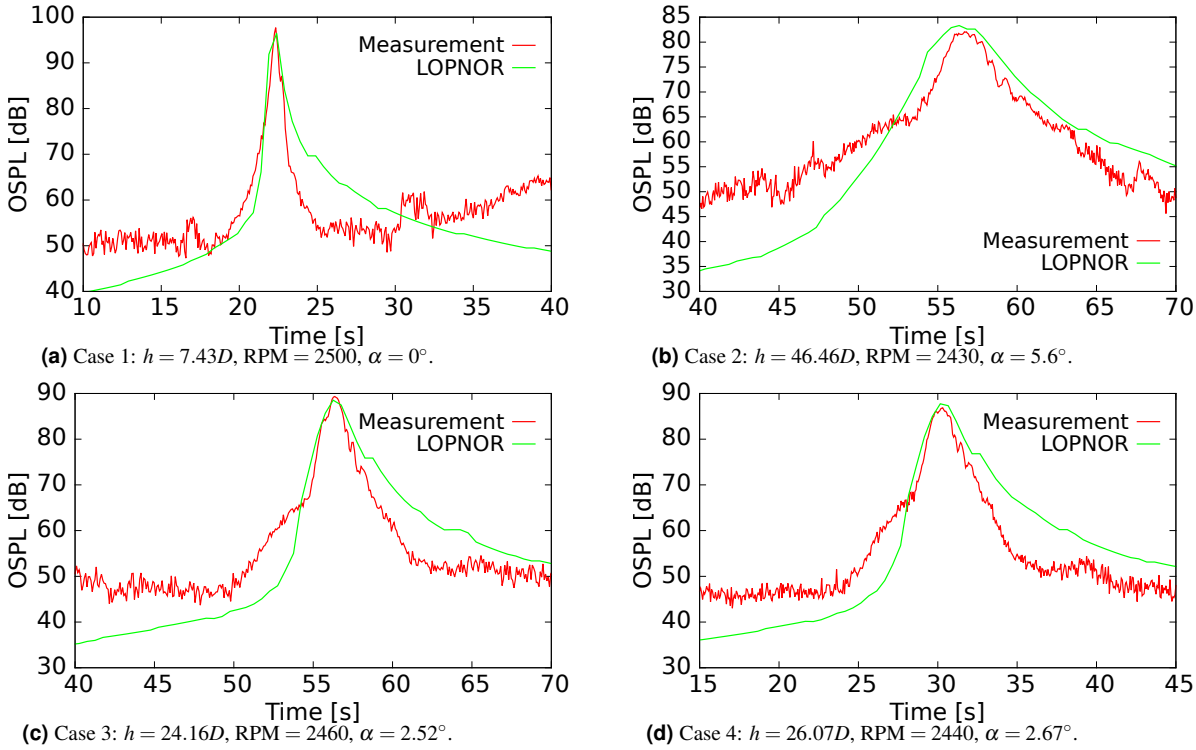

(a) Case 1: $h = 7.43D$, RPM $= 2500$, $\alpha = 0°$.

(b) Case 2: $h = 46.46D$, RPM $= 2430$, $\alpha = 5.6°$.

(c) Case 3: $h = 24.16D$, RPM $= 2460$, $\alpha = 2.52°$.

(d) Case 4: $h = 26.07D$, RPM $= 2440$, $\alpha = 2.67°$.

Figure 10: Comparison of time-level history of flyover noise predicted with the LOPNOR tool and outdoor measurements. The parameter h indicates the source-receiver distance in terms of rotor diameter D. Case 1 corresponds to a constant-altitude level flight, while the other cases represent take-off flights with varying climb angle α.

The second one is based on the frequency-domain solution of the Ffowcs Williams-Hawkings (FW-H) integral equation applied to a radial distribution of acoustically non-compact sources (Ghorbaniasl, Huang, Siozos-Rousoulis, & Lacor, 2015). This formulation is advantageous compared to the abovementioned Hanson's formulation, as well as the widely-used FW-H formulations, such as Farassat 1 and 1A, as it accounts for the acoustic effects of incoming flow with arbitrary direction (3D), whereas both formulations of Farassat 1 and 1A, without introducing algorithmic modification (Farassat, Dunn, & Spence, 1992), cannot be directly employed to account for non-axial inflow effects with 3D varying inflow direction. In our recent work (Yunus, Casalino, Romani, & Snellen, 2024), this formulation was implemented in LOPNOR and coupled with an extended BEMT procedure, accounting for the unsteadiness due to the variation in the inflow direction, to predict propeller noise at incidence.

LOPNOR predictions showed good agreement with both experimental measurements and high-fidelity simulations as shown in Fig. 11.

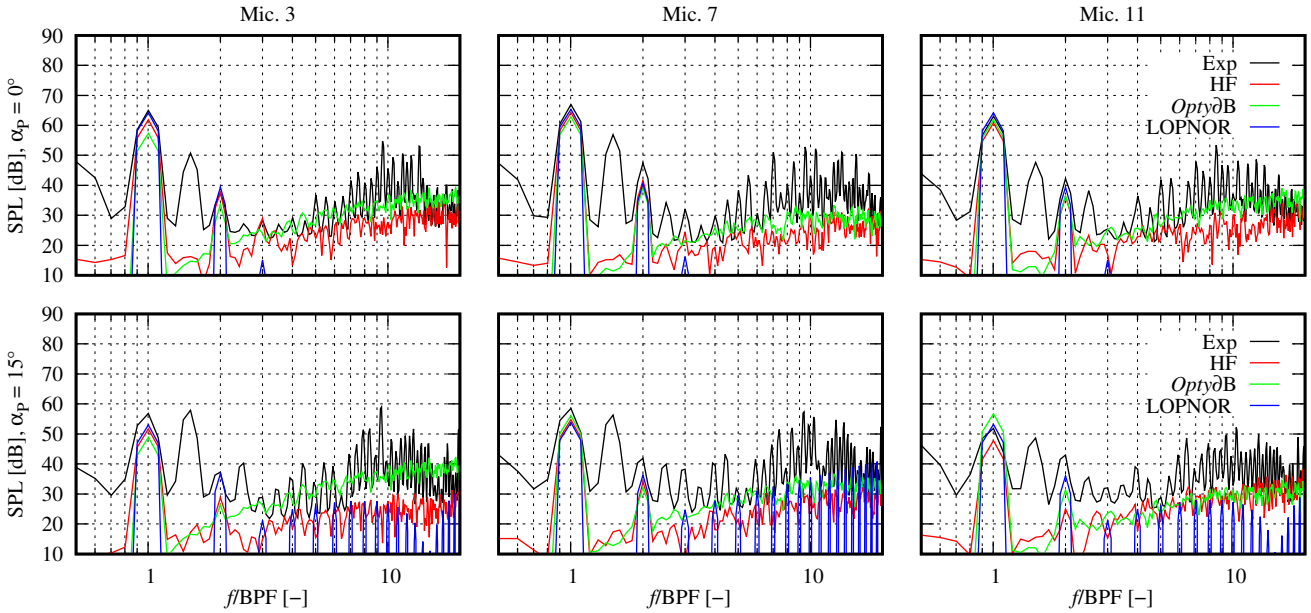

Figure 11: Far-field noise spectra for three microphones and both axial (top) and non-axial flow conditions (bottom).

The works mentioned above highlight the noise prediction capabilities for a single propeller under both axial and non-axial inflow conditions. However, aerodynamic interactions between adjacent rotors can significantly impact noise generation (Zarri, Dell'Erba, Munters, & Schram, 2022), depending on the operating conditions and rotor placement configurations. Considerable efforts are underway to model noise generated by rotor-rotor and rotor-airframe interactions. In the near future, LOPNOR will be further enhanced to improve the accuracy of drone noise predictions by incorporating rotor-rotor and rotor-airframe interactions, as well as accounting for acoustic scattering from airframes.

Moreover, accurate prediction of noise propagation in an urban environment is challenging as various wave phenomena, i.e., multiple reflections, diffraction, refraction, and propagation scenarios, such as standing waves with large amplitude oscillations in narrow urban canyons and scattering by atmospheric turbulence, should be accounted for. Over the years, various computational tools have been developed to simulate the propagation of outdoor noise. Although wave-based models directly solve the convected wave equation and offer high-fidelity results, they become computationally prohibitive as the source frequency and the propagation distance increase. Consequently, ray acoustics, based on high-frequency approximations of the convected wave equation, has emerged as a more practical and efficient approach to simulate outdoor noise propagation (Yunus, Casalino, Avallone, & Ragni, 2023a). In our PB approach, the drone noise propagation is modeled using the ray acoustics method combined with a Gaussian beam summation technique, which accounts for multiple reflections over three-dimensional terrain surfaces and atmospheric refraction due to variations in wind velocity and temperature profiles in both horizontal and vertical directions. This approach is implemented in our acoustic ray and Gaussian beam propagation solver, UYGUR. A schematic of the computational procedure is shown in Fig. 12. Further details on the solver and modelling approach can be found in (Yunus et al., 2023a; Yunus, Casalino, Avallone, & Ragni, 2023b; Yunus, 2023).

UYGUR has been validated against the full-wave solution of a finite element method (FEM) based solver. Figure 13 compares the prediction from UYGUR against the FEM solver, demonstrating both computational efficiency and acceptable accuracy (Yunus et al.,

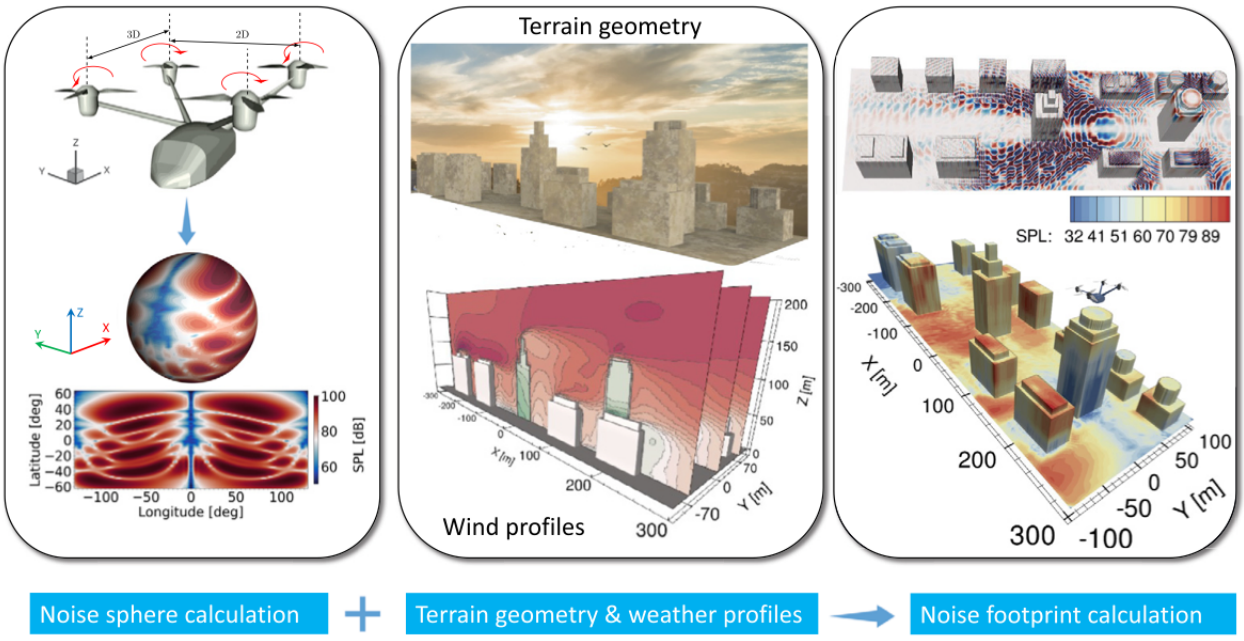

Figure 12: Schematic illustration of the computational procedure in UYGUR.

2023a).

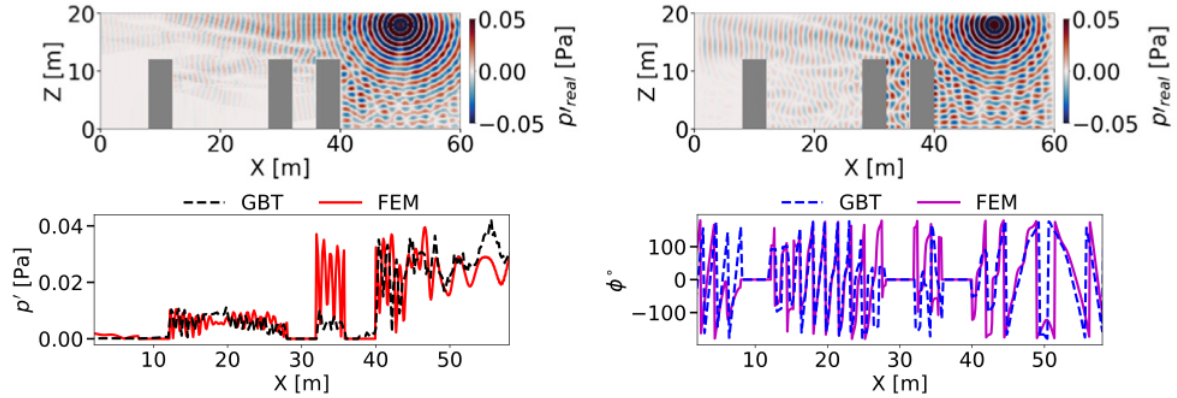

Figure 13: Comparison of acoustic wave fields on a vertical plane containing a three-building urban setting predicted with UYGUR (left) and a FEM-based solver (right). Pressure magnitude (bottom left) and phase (bottom right) along a line at $Z = 10$ m above the ground.

Previously, UYGUR has been applied to investigate vertiport noise from hovering drones near high-rise buildings (Yunus et al., 2023b), as well as the noise footprint of maneuvering flights in vertiport settings that resemble typical urban environments (Yunus, Varriale, & Snellen, 2024). Future work will validate UYGUR against field measurements and extend it to study the effects of building-induced turbulence on drone noise propagation in urban settings.

4. Human perception

Recent studies (Merino-Martinez et al., 2021; Merino-Martinez, Pieren, Schäffer, & Simons, 2022; Merino-Martinez, Yupa-Villanueva, von den Hoff, & Pockelé, 2024) showed that Sound Quality Metrics (SQMs) based on perception describe the subjective perception of sound by human hearing in a better way compared to conventional sound metrics typically employed in noise assessment, such as $L_{\mathrm{p,A,eq}}$, which essentially quantifies the physical magnitude of sound based on pressure fluctuations. Therefore, there is a growing interest in psychoacoustic studies involving SQMs and listening experiments (Gwak et al., 2020; Schade et al.,

2024; Torija, Ramos-Romero, & Green, 2024) to capture the auditory behavior of the human ear more accurately.

4.1 Psychoacoustic sound quality metrics

The five most commonly used SQMs (Greco et al., 2023) are:

- Loudness (N): Subjective perception of sound magnitude corresponding to the overall sound intensity (*ISO norm 532–1 – Acoustics – Method for calculating loudness – Zwicker method*, 2017).
- Tonality (K): Measurement of the perceived strength of unmasked tonal energy within a complex sound (Aures, 1985).
- Sharpness (S): Representation of the high-frequency sound content (von Bismark, 1974).
- Roughness (R): Hearing sensation caused by sounds with modulation frequencies between 15 Hz and 300 Hz (Daniel & Webber, 1997).
- Fluctuation strength (FS): Assessment of slow fluctuations in loudness with modulation frequencies up to 20 Hz, with maximum sensitivity for modulation frequencies around 4 Hz (Osses, García León, & Kohlrausch, 2016).

These five SQMs are typically calculated for each drone flyover recording and their 5% percentile values are normally considered, representing the value of each SQM exceeded 5% of the total recording time. These 5% percentile values can then be combined into global psychoacoustic annoyance (PA) metrics, following models like those outlined by Zwicker (Fastl & Zwicker, 2007), More (More, 2010), and Di *et al.* (Di, Chen, Song, Zhou, & Pei, 2016). The open-source MATLAB toolbox SQAT (Sound Quality Analysis Toolbox) v1.1 (Greco et al., 2023; Greco, G. F. and Merino-Martinez, R. and Osses, A., 2024) is employed to calculate these SQMs, PA metrics, and conventional sound metrics (e.g. equivalent A-weighted sound pressure level $L_{\mathrm{p,A,eq}}$, sound exposure level $L_{\mathrm{p,A,e}}$, and effective perceived noise level (EPNL)). This toolbox enables a quick calculation of these metrics for any input sound signal. The GitHub repository of this toolbox can be found in (Greco, G. F. and Merino-Martinez, R. and Osses, A., 2023).

Recently, another sound quality metric called impulsiveness (I) is also being considered in drone noise assessments (Green et al., 2024). The model proposed by Willemsen and Rao (Willemsen & Rao, 2010) assesses the loudness N over time to quantify the degree of impulsive content within a sound. The cumulative impulse content denoted I_{N}, can also be calculated to calculate the PA metric proposed by the same authors (Willemsen & Rao, 2010). The code implementation of the impulsiveness and PA metric by Willemnsen and Rao is intended to be soon included in the SQAT repository.

Recent publications assessed the SQM and PA values of flyover field recordings of different drone types. Yupa-Villanueva *et al.* (Yupa-Villanueva, Merino-Martinez, Altena, & Snellen, 2024) explored the SQMs through density traces of their instantaneous and their 5% percentiles values, as shown in Fig. 14. Sharpness, tonality, roughness, and impulsiveness exhibit similar transient density trace patterns, suggesting a consistent auditory signature across these attributes. However, loudness and fluctuation strength did not demonstrate comparable transient density patterns. In terms of perceived attributes, the heaviest drone was characterized as the 'harshest', 'least sharp', and 'quietest'. Conversely, the lightest drone is perceived as the 'sharpest', 'least harsh', and 'least impulsive'. The drone with the lowest installation ratio (d/D, where d is the diagonal distance between each propeller and D

is the propeller diameter) was found to be the 'loudest', 'most tonal', 'most beating', and 'most impulsive'. Additionally, one of the drones with the largest propeller diameter is perceived as the 'least tonal'. An analysis considering single values of psychoacoustic annoyance using the previous PA models indicated that the drone with the lowest d/D was perceived as the most annoying, while the heaviest drone was assessed as the least annoying. Additionally, the Willemsen and Rao PA model predicted higher annoyance values in comparison to other PA models, as shown in table Table 1.

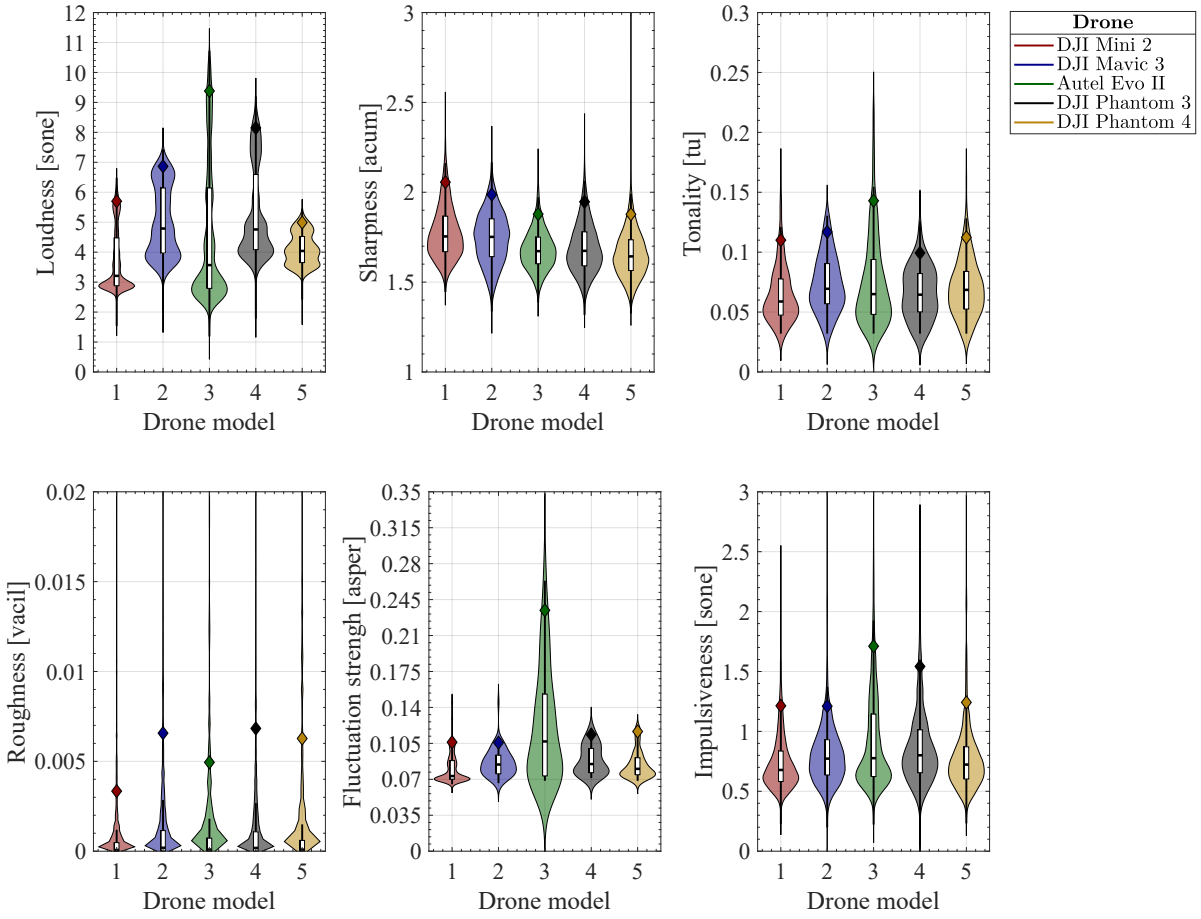

Figure 14: Density traces of instantaneous values of sound quality metrics and their 5% percentile values.

Table 1: Summary of normalized psychoacoustic annoyance (PA) values predicted by the Zwicker, More, Di et al., and Willsemsen and Rao models.

Drone number	Drone model	Normalized annoyance [-]			
		Zwicker	More	Di et al.	Willemsen and Rao
1	DJI Mini 2	0.60	0.50	0.55	0.87
2	DJI Mavic 3	0.72	0.60	0.67	0.92
3	Autel EVO II	1	1	1	1
4	DJI Phantom 3	0.86	0.71	0.78	0.96
5	DJI Phantom 4	0.51	0.44	0.48	0.84

In another study, Yupa-villanueva *et al.* (Yupa-Villanueva, Merino-Martinez, Andino Cappagli, Altena, & Snellen, 2024) studied four types of drones (single-propeller quadcopter, coaxial-propeller quadcopter, quadplane eVTOL, and tailsitter eVTOL) and the the SQMs revealed (Fig. 15) that the coaxial-propeller quadcopter was deemed the loudest, whereas the tailsitter eVTOL was evaluated as the quietest, albeit notably sharp. Tonality perception varied among the drones, with the quadplane eVTOL rated as the most tonal and the tailsitter as

the least one. The single-propeller quadcopter was perceived as emitting the harshest and most beating sound. Regarding impulsiveness, the coaxial-propeller quadcopter was considered the most impulsive, whereas the tailsitter was the least impulsive. Figure 16 presents the psychoacoustic annoyance using the model by Di et al. (Di et al., 2016) for each drone. The coaxial propeller-equipped drone reveals an annoyance prediction of 71.8 units, while the single propeller quadcopter achieves 24.5 units, making the coaxial-propeller-equipped drone approximately three times more annoying. Comparing eVTOL vehicles, the quadplane is also approximately three times more annoying than the tailsitter, with annoyance values of 9 and 3.2 units, respectively. Nevertheless, the eVTOL vehicles present considerably lower psychoacoustic annoyance values.

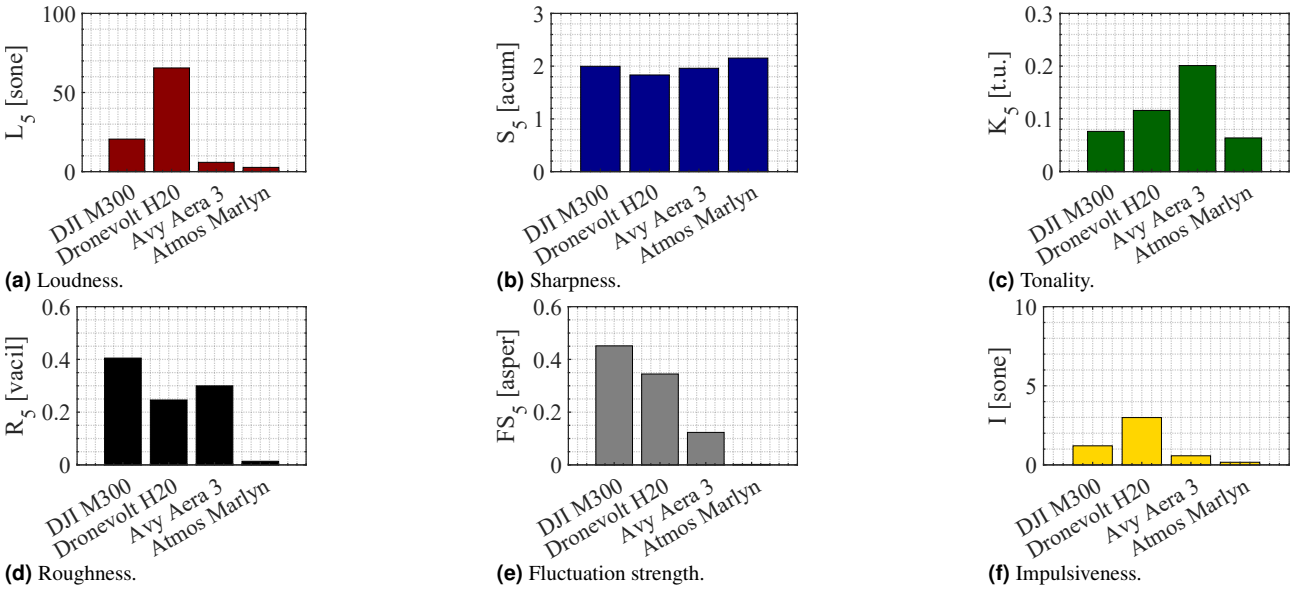

(a) Loudness. **(b)** Sharpness. **(c)** Tonality. **(d)** Roughness. **(e)** Fluctuation strength. **(f)** Impulsiveness.

Figure 15: 5% percentile values of the sound quality metrics.

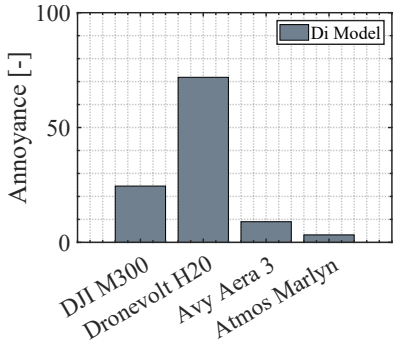

Figure 16: Predicted psychoacoustic annoyance for each drone using the Di model.

A recent study (Merino-Martinez, Ben-Gida, & Snellen, 2024) related to the perception-influenced design (see Fig. 1) and noise assessment of drone propellers modified the geometry of a baseline APC $14'' \times 5.5''$ two-bladed propeller, see Fig. 17(a), to minimize the perceived noise annoyance while maintaining its aerodynamic performance. The multi-disciplinary optimization technique employed was performed using the getPROP framework (Kvurt, Ruf, Hertzman, Stalnov, & Ben-Gida, 2023), which consists of various modules, such as aerodynamic modelling, performance computation, aeroacoustic prediction, atmospheric attenuation, psychoacoustics, and multi-objective optimization. The chord and twist angle radial distributions of both propellers are presented in Fig. 17(a). Both propellers had a radius of 177.8 mm and a design thrust point of 9.5 N. The blade sections of the baseline propeller consist of a NACA5608 airfoil shape, whereas a low-Reynolds FX$63-137$ airfoil was

selected for the optimized propeller design to improve its performance in the low-Reynolds number regime (Selig, 2003). The noise emissions of both propellers were measured in a fully-anechoic chamber with a cut-off frequency of $150\,$Hz using a directivity arc consisting of fifteen microphones placed at a radial distance of 1.5 m from the propeller hub. The circular arc spanned an azimuth angular range of $0° < \theta < 105°$, where $\theta = 0°$, corresponds to the axis of rotation above the propeller's hub, whereas $\theta = 90°$ refers to the rotor disk plane, see the schematic propeller test rig depicted in Fig. 17(b). For further details on the experimental setup, the interested reader is referred to (Merino-Martinez, Ben-Gida, & Snellen, 2024).

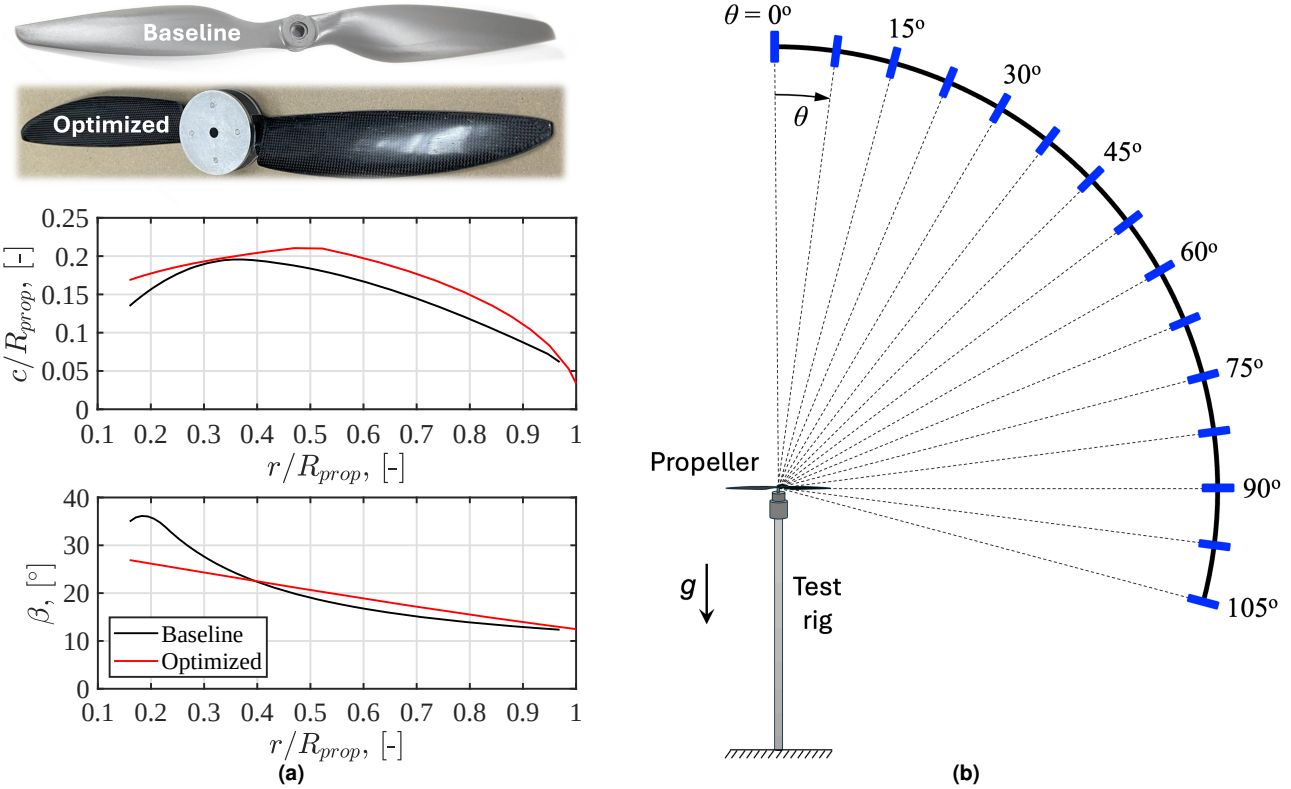

Figure 17: (a) Top: Photographs of both propellers. Center: Radial distribution of the blade's normalized chord (c/R_{prop}), and Bottom: pitch angle (β), for the reference propeller (black) and the optimal design propeller (red). (b) Schematics of the experimental setup employed, consisting of the propeller test rig and the circular arc array.

A preliminary analysis with conventional sound metrics showed noise reductions of about 2 to 3 dBA in the overall A-weighted sound pressure level for the optimized propeller. The attenuation was especially noticeable for the high-frequency range, where reductions of about 9 dBA were reported. Figure 18 depicts the directivity plots for different psychoacoustic metrics. As expected from the aforementioned reduction in high-frequency noise, the optimized propeller shows notable reductions in sharpness (S_5, Fig. 18(a)) up to 0.47 acum. The tonality (K_5, Fig. 18(b)) presents considerably high values (up to 0.25 t.u. for the baseline case) and maximum values on the propeller plane ($\theta \approx 90°$). The optimized propeller appears to reduce the tonality to almost half its baseline value in that direction. This reduction is explained by the generally lower tones observed for this design and higher masking by broadband noise, especially at low frequencies. This phenomenon could be explained by the expected reduction in leading-edge noise (blade-vortex interaction) for the optimized case. Lastly, the global psychoacoustic annoyance (PA) metric presents consistent reductions up to 20% in all the emission directions investigated. All in all, these results seem to indicate that the optimized propeller does indeed provide substantial reductions in noise annoyance for the same thrust condition. Additional results referring to other SQMs are included in

(Merino-Martinez, Ben-Gida, & Snellen, 2024).

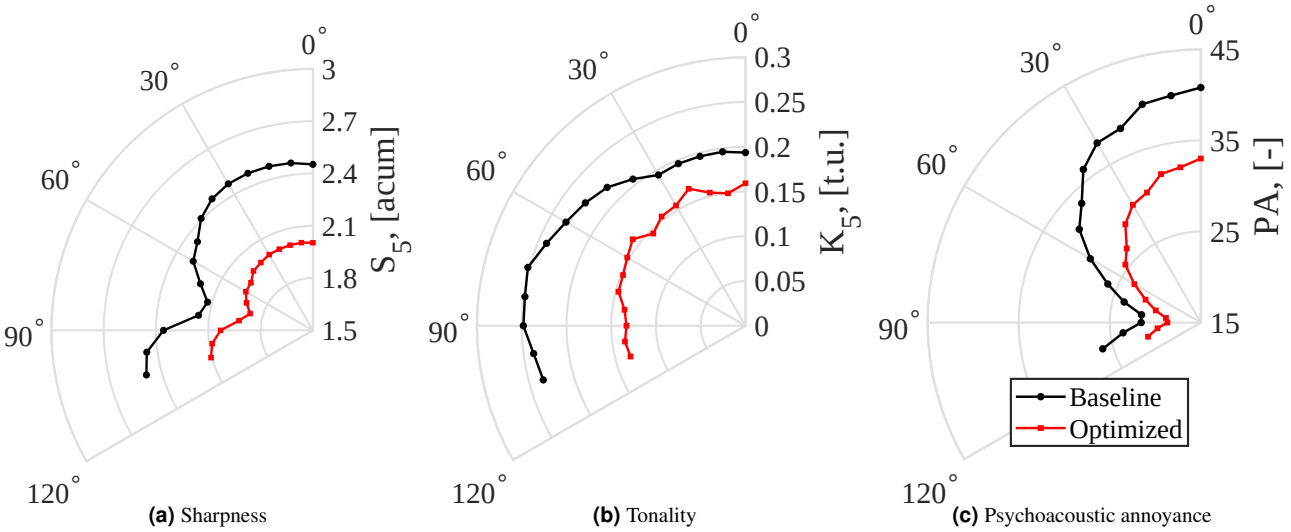

(a) Sharpness **(b)** Tonality **(c)** Psychoacoustic annoyance

Figure 18: Directivity plots for both propellers considering different sound metrics: (a) sharpness, (b) tonality, and (c) psychoacoustic annoyance.

Additional research examples also employed psychoacoustic metrics and sound auralization to assess the noise footprint of full-scale UAM vehicles (Schade et al., 2024) and commercial aircraft (Thoma et al., 2024; Merino-Martinez, Besnea, von den Hoff, & Snellen, 2024).

4.2 Listening experiments

Conducting psychoacoustic listening experiments with human subjects is crucial for obtaining valuable information on the perceptual aspects of different designs of drones and UAM vehicles, as well as their operational conditions and other factors.

The recently-developed Psychoacoustic Listening Laboratory (PALILA) at the Faculty of Aerospace Engineering of TU Delft (Merino-Martinez et al., 2023) consists of a box-in-box soundproof booth with interior dimensions of 2.32 m (length) $\times$ 2.32 m (width) $\times$ 2.04 m (height). The interior walls, ceiling, and part of the floor are covered with acoustic-absorbing foam panels to prevent sound reflections, see Fig 19(a). This results in free-field sound propagation conditions for frequencies higher than or equal to 1600 Hz and a reverberation time of only 0.07 s. The walls of PALILA consist of a sandwich structure, which provides a weighted average transmission loss of 45 dB. The A-weighted overall background noise level is 13.4 dBA. The listening room is equipped with a Dell Latitude 7340 touchscreen laptop and a pair of calibrated Sony WH-1000XM4 over-ear, closed-back headphones, for sound reproduction and participant interaction. Participants record their subjective responses to the sounds using a Python-based graphical user interface (GUI) for listening experiments (Pockelé, 2024), see Fig 19(b).

A recent investigation (Merino-Martinez, Yupa-Villanueva, et al., 2024) assessed the performance of different sound metrics and PA models in predicting the noise annoyance ratings from a psychoacoustic listening experiment with 57 participants and featuring the acoustic recordings of nine different drones of different topologies (see Figs. 14 and 15), including six quadcopters with single propellers, a quadcopter with counterrotating propellers, and two types of hybrid eVTOL drones, see Fig. 8. Table 2 shows the correlation coefficients ρ and the respective p-values of the correlations reported between each metric and the mean annoyance ratings. For this particular experiment, it seems that the PA models of Zwicker ($\rho = 0.857$, p-value = 0.003) and Willemsen and Rao ($\rho = 0.856$, p-value = 0.003) outperform the rest of the alternative metrics considered, especially EPNL ($\rho = 0.777$, p-value = 0.014).

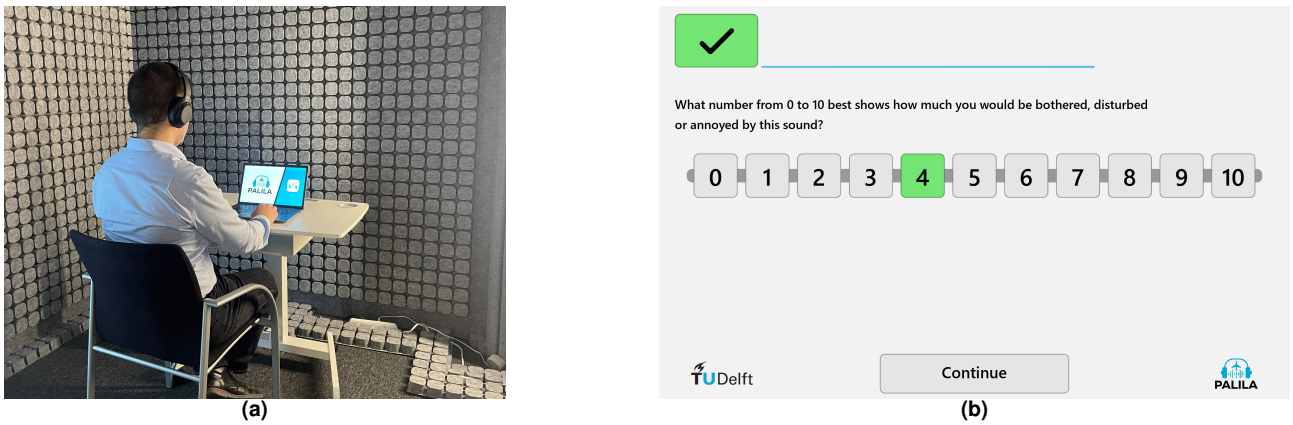

(a) (b)

Figure 19: Examples of (a) a listening experiment inside PALILA and (b) the graphical user interface (GUI).

For illustration purposes, the correlation analyses for EPNL and the PA model of Zwicker are presented in Fig. 20.

Table 2: Correlation coefficients and associated p-values reported for the different sound metrics and psychoacoustic annoyance models for the drone noise psychoacoustic experiments.

Metric / model	ρ	**p-value**
$L_{\mathrm{p,A,eq}}$	0.807	0.009
$L_{\mathrm{p,A,e}}$	0.808	0.008
EPNL	0.777	0.014
PA (Zwicker)	**0.857**	**0.003**
PA (More)	0.828	0.006
PA (Di *et al.*)	0.834	0.005
PA (Willemsen and Rao)	0.856	0.003

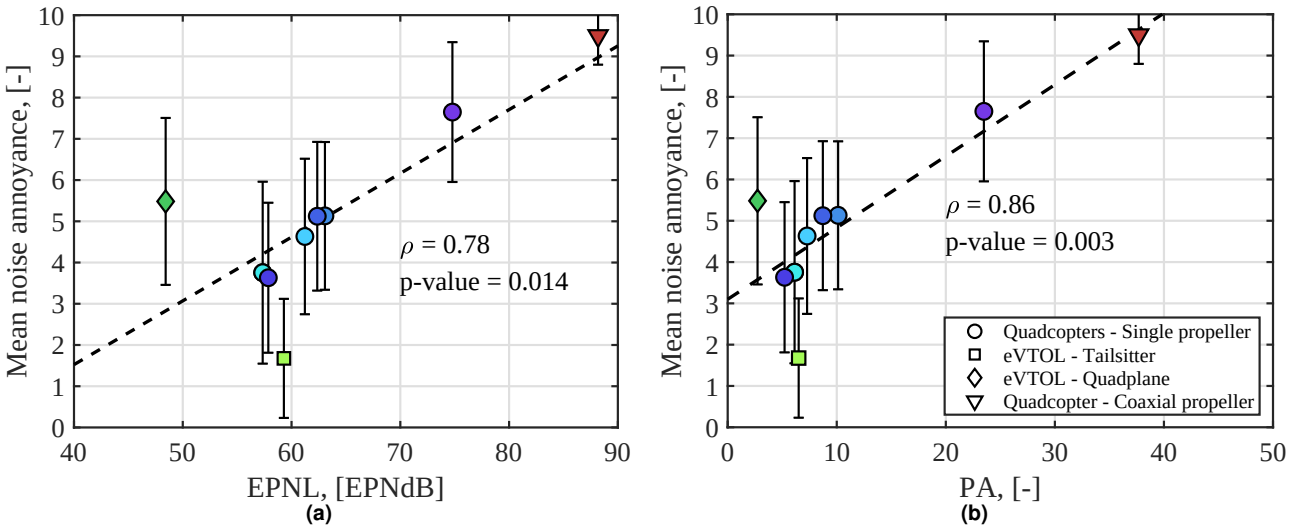

(a) (b)

Figure 20: Mean noise annoyance ratings per drone type with respect to (a) EPNL and (b) PA (Zwicker's model). The error bars denote the standard deviations in the annoyance ratings. The respective least-squares linear fits for all drones are plotted as dashed black lines, including the correlation coefficient ρ and p-value.

5. CONCLUSIONS

An overview of the recent and ongoing research work in the fields of drone and UAM vehicle noise at TU Delft has been provided in this manuscript. In particular, representative examples of aeroacoustic measurements (both in field experiments and in wind-tunnel facilities), noise modelling (employing both data-driven and physics-based methods), and human perception (including analyses with psychoacoustic metrics and listening experiments) were provided. These three main pillars are all essential for achieving perception-based design and noise assessment of drones, UAM vehicles, and their components, in order to achieve devices that cause the minimum disturbance to the living environment.

This research topic is currently a vibrant environment with rapid developments and promising results. Some current challenges include:

- Accounting for the scalability and installation effects to convert results from scaled wind-tunnel experiments to full-scale geometries is essential to device noise mitigation strategies.
- Achieving efficient and accurate noise prediction models for drones and UAM vehicles. In addition, to assess the perceptual characteristics of the modelled sounds, realistic auralization techniques that provide plausible results are essential.
- Assessing the influence of topological (e.g. geometric design), operational (e.g. flight dynamics), and environmental (e.g. signal-to-noise ratio) conditions in human perception. This is particularly important since drones and UAM vehicles present considerably different sound signatures than other environmental noise sources.

ACKNOWLEDGMENTS

This publication conveys some results that belong to the following research projects:

1. The *Listen to the future* project (No. 20247) of the research programme Veni 2022 (Domain Applied and Engineering Sciences) granted to Roberto Merino-Martinez, which is (partly) financed by the Dutch Research Council (NWO).
2. The *HOPE* (Hydrogen Optimized multi-fuel Propulsion system for clean and silEnt aircraft) project, which has received funding from the European Union's Horizon Europe research and innovation programme under grant agreement No. 101096275.
3. The *REFMAP* (Reducing Environmental Footprint through Transformative Multi-scale Aviation Planning) project, which has received funding from the European Union's Horizon Europe research and innovation programme under grant agreement No. 101096698.
4. The *ENODISE* (ENabling Optimized Disruptive Airframe-Propulsion Integration Concepts) project, which has received funding from the European Union's Horizon 2020 research and innovation programme under grant agreement No. 860103.
5. The *IMAFUSA* (IMpact and capacity Assessment Framework for U-space Societal Acceptance) project, which has received funding from the SESAR 3 joint undertaking under grant agreement number 101114776.
6. The *ACTION* (ACoustic detecTION of class I (<20 kg) unmanned aircraft systems supported by optical sensors) project, which has received funding from the Dutch Ministry of Defence under Nationaal Technologie Project (NTP) N21/005.

REFERENCES

Allen, C. S., Blake, W. K., Dougherty, R. P., Lynch, D., Soderman, P. T., & Underbrink, J. R. (2002). *Aeroacoustic Measurements* (T. J. Mueller, Ed.). Berlin, Heidelberg: Springer Berlin Heidelberg. doi: 10.1007/978-3-662-05058-3

Altena, A., Luesutthiviboon, S., Croon, G. D., Snellen, M., & Voskuijl, M. (2023, 7). Comparison of acoustic localisation techniques for drone position estimation using real-world experimental data. In *Proceedings of the 29th international congress on sound and vibration* (p. 1-8).

Amiri-Simkooei, A., Tiberius, C., & Lindenbergh, R. (2024). Deep learning in standard least-squares theory of linear models: Perspective, development and vision. *Engineering Applications of Artificial Intelligence*, *138*, 109376.

Aures, W. (1985). Procedure for calculating the sensory euphony of arbitrary sound signal. In German: Berechnungsverfahren für den sensorischen Wohlklang beliebiger Schallsignale. *Acustica*, *59*(2), 130–141. Retrieved from https://www.ingentaconnect.com/contentone/dav/aaua/1985/00000059/00000002/art00008

Awad, M., & Khanna, R. (2015). Support vector regression. *Efficient learning machines*, 67–80.

Baars, W. J., & Ragni, D. (2024, September). Low-Frequency Intensity Modulation of High-Frequency Rotor Noise. *AIAA Journal*, *62*(9), 3374–3390. doi: 10.2514/1.J063610

Bazilinskyy, P., Merino-Martinez, R., Özcan, E., Dodou, D., & de Winter, J. C. F. (n.d.). Exterior sounds for electric and automated vehicles: Loud is effective. , *214*(109673), 1–13. Retrieved from https://doi.org/10.1016/j.apacoust.2023.109673 doi: 10.1016/j.apacoust.2023.109673

Bento, H., VanderCreek, C., Avallone, F., Ragni, D., Sijtsma, P., & Snellen, M. (2023). Wall treatments for aeroacoustic measurements in closed wind tunnel test sections. In *29^{th} aiaa/ceas aeroacoustics conference, june 12 – 16 2023, san diego, ca, usa.* Retrieved from http://arc.aiaa.org/doi/pdf/10.2514/6.2023-4162 (AIAA paper 2023–4162) doi: 10.2514/6.2023-4162

Breiman, L. (2001). Random forests. *Machine learning*, *45*(1), 5–32.

Casalino, D., Grande, E., Romani, G., Ragni, D., & Avallone, F. (2021, June). Definition of a benchmark for low Reynolds number propeller aeroacoustics. *Aerospace Science and Technology*, *113*. doi: 10.1016/j.ast.2021.106707

Daniel, P., & Webber, R. (1997). Psychoacoustical Roughness: Implementation of an Optimized Model. *Accustica – acta acustica*, *83*, 113–123. Retrieved from https://www.ingentaconnect.com/contentone/dav/aaua/1997/00000083/00000001/art00020

Di, G.-Q., Chen, X.-W., Song, K., Zhou, B., & Pei, C.-M. (2016). Improvement of Zwicker's psychoacoustic annoyance model aiming at tonal noises. *Applied Acoustics*, *105*, 164–170. Retrieved from http://dx.doi.org/10.1016/j.apacoust.2015.12.006 doi: 10.1016/j.apacoust.2015.12.006

Dreier, C., & Vorländer, M. (2024). Drone auralization model with statistical synthesis of amplitude and frequency modulations. *Acta Acustica*, *8*(35), 1–13. Retrieved from https://doi.org/10.1051/aacus/2024026 doi: 10.1051/aacus/2024026

Ezugwu, E., Fadare, D., Bonney, J., Da Silva, R., & Sales, W. (2005). Modelling the correlation between cutting and process parameters in high-speed machining of Inconel 718 alloy using an artificial neural network. *International Journal of Machine Tools and Manufacture*, *45*(12-13), 1375–1385.

Farassat, F., Dunn, M., & Spence, P. (1992). Advanced propeller noise prediction in the time domain. *AIAA journal*, *30*(9), 2337–2340.

Fastl, H., & Zwicker, E. (2007). *Psychoacoustics – Facts and models* (Third ed.). Springer Series in Information Sciences. Retrieved from https://www.springer.com/gp/book/9783540231592 (ISBN: 987–3–540–68888–4)

Ghorbaniasl, G., Huang, Z., Siozos-Rousoulis, L., & Lacor, C. (2015). Analytical acoustic pressure gradient prediction for moving medium problems. *Proceedings of the Royal Society A: Mathematical, Physical and Engineering Sciences*, *471*(2184), 20150342.

Grande, E., Romani, G., Ragni, D., Avallone, F., & Casalino, D. (2022, February). Aeroacoustic Investigation of a Propeller Operating at Low Reynolds Numbers. *AIAA Journal*, *60*(2), 860–871. doi: 10.2514/1.J060611

Greco, G. F., Merino-Martinez, R., Osses, A., & Langer, S. C. (2023). SQAT: a MATLAB-based toolbox for quantitative sound quality analysis. In 52^{th} *international congress and exposition on noise control engineering, august 20 – 23 2023, chiba, greater tokyo, japan.* International Institute of Noise Control Engineering (I-INCE). Retrieved from https://www.researchgate.net/publication/373334884_SQAT_a_MATLAB-based_toolbox_for_quantitative_sound_quality_analysis

Greco, G. F. and Merino-Martinez, R. and Osses, A. (2023, May). *SQAT: a sound quality analysis toolbox for MATLAB.* Retrieved from https://github.com/ggrecow/sqat (Accessed in May 2023)

Greco, G. F. and Merino-Martinez, R. and Osses, A. (2024, May). *SQAT: a sound quality analysis toolbox for MATLAB (version v1.1).* Retrieved from https://zenodo.org/records/10580337 (Accessed in May 2024) doi: 10.5281/zenodo.10580337

Green, N., Torija, A. J., & Ramos-Romero, C. (2024, February). Perception of noise from unmanned aircraft systems: Efficacy of metrics for indoor and outdoor listener positions. *Journal of the Acoustical Society of America*, *155*(2), 915–929. Retrieved from http://dx.doi.org/10.1121/10.0024522 doi: 10.1121/10.0024522

Gwak, D. Y., Han, D., & Lee, S. (2020, December). Sound quality factors influencing annoyance from hovering UAV. *Journal of Sound and Vibration*, *489*, 115651. Retrieved from https://doi.org/10.1016/j.jsv.2020.115651 doi: 10.1016/j.jsv.2020.115651

Hanson, D. (1990). Noise radiation of propeller loading sources with angular inflow. In *13th aeroacoustics conference* (p. 3955).

Heutschi, K., Ott, B., Nussbaumer, T., & Wellig, P. (2020, October). Synthesis of real world drone signals based on lab recordings. *Acta Acoustica*, *4*(24), 1–10. Retrieved from http://dx.doi.org/10.1051/aacus/2020023 doi: 10.1051/aacus/2020023

ISO norm 532–1 – Acoustics – Method for calculating loudness – Zwicker method (Tech. Rep. No. 1). (2017). International Organization for Standardization. Retrieved from https://www.iso.org/obp/ui/#iso:std:iso:532:-1:ed-1:v2:en

Kvurt, A., Ruf, D., Hertzman, O., Stalnov, O., & Ben-Gida, H. (2023). getPROP - A MATLAB suite for low-noise signature propeller design, analysis, and optimization. In *Aiaa scitech forum, 23-27 january, national harbor, md & online.* doi: 10.2514/6.2023-0026

Magliozzi, B., Hanson, D., & Amiet, R. (1991). Propeller and propfan noise. In *Hubbard hh, editor. aeroacoustics of flight vehicles: theory and practice* (pp. 1–64). NASA.

Merino-Martinez, R. (2018). *Microphone arrays for imaging of aerospace noise sources* (Doctoral dissertation, Delft University of Technology). (ISBN: 978–94–028–1301–2) doi: 10.4233/uuid:a3231ea9-1380-44f4-9a93-dbbd9a26f1d6

Merino-Martinez, R. (2024). Guidelines for Accurate Sound Source Quantification in Closed–Section Wind Tunnels. In 10^{th} *berlin beamforming conference, june 10 – 11 2024, berlin, germany.* GFaI, e.V., Berlin. Retrieved from https://www.bebec.eu/fileadmin/bebec/downloads/bebec-2024/papers/BeBeC-2024-S04.pdf (BeBeC–2024–S04)

Merino-Martinez, R., Ben-Gida, H., & Snellen, M. (2024). Psychoacoustic Evaluation of an Optimized Low–Noise Drone Propeller Design. In 30^{th} *international congress on sound and vibration (icsv), july 8 – 11 2024, amsterdam, the netherlands.*

Merino-Martinez, R., Besnea, I., von den Hoff, B., & Snellen, M. (2024). Psychoacoustic Analysis of the Noise Emissions from the Airbus A320 Aircraft Family and its Nose Landing Gear System. In 30^{th} *aiaa/ceas aeroacoustics conference, june 4 – 7 2024, rome, italy.* Retrieved from http://arc.aiaa.org/doi/pdf/10.2514/6.2024-3398 (AIAA paper 2024–3398) doi: 10.2514/6.2024-3398

Merino-Martinez, R., Heblij, S. J., Bergmans, D. H. T., Snellen, M., & Simons, D. G. (2019). Improving Aircraft Noise Predictions by Considering the Fan Rotational Speed. *Journal of Aircraft*, *56*(1), 284–294. Retrieved from http://arc.aiaa.org/doi/abs/10.2514/1.C034849 doi: 10.2514/1.C034849

Merino-Martinez, R., Pieren, R., & Schäffer, B. (2021, May). Holistic approach to wind turbine noise: From blade trailing–edge modifications to annoyance estimation. *Renewable and Sustainable Energy Reviews*, *148*(111285), 1–14. Retrieved from https://doi.org/10.1016/j.rser.2021.111285 doi: 10.1016/j.rser.2021.111285

Merino-Martinez, R., Pieren, R., Schäffer, B., & Simons, D. G. (2022). Psychoacoustic model for predicting wind turbine noise annoyance. In 24^{th} *international congress on acoustics (ica), october 24 – 28 2022, gyeongju, south korea.* Retrieved from https://www.researchgate.net/publication/364996997_Psychoacoustic_model_for_predicting_wind_turbine_noise_annoyance

Merino-Martinez, R., Sijtsma, P., Snellen, M., Ahlefeldt, T., Antoni, J., Bahr, C. J., ... Spehr, C. (2019, March). A review of acoustic imaging methods using phased microphone arrays (part of the Aircraft Noise Generation and Assessment special issue). *CEAS Aeronautical Journal*, *10*(1), 197–230. Retrieved from https://link.springer.com/article/10.1007/s13272-019-00383-4 doi: 10.1007/s13272-019-00383-4

Merino-Martinez, R., von den Hoff, B., & Simons, D. G. (2023). Design and acoustic characterization of a psychoacoustic listening facility. In 29^{th} *international congress on sound and vibration (icsv), july 9 – 13 2023, prague, czech republic.* Retrieved from https://www.researchgate.net/publication/372235624_Design_and_Acoustic_Characterization_of_a_Psychoacoustic_Listening_Facility

Merino-Martinez, R., Yupa-Villanueva, R. M., von den Hoff, B., & Pockelé, J. S. (2024). Human response to the flyover noise of different drones recorded in field measurements. In 3^{rd} *quiet drones conference, september 8 – 11 2024, manchester, united kingdom.*

Merino-Martínez, R., Rubio Carpio, A., Lima Pereira, L. T., Van Herk, S., Avallone, F., Ragni, D., & Kotsonis, M. (2020, December). Aeroacoustic design and characterization of the 3D-printed, open-jet, anechoic wind tunnel of Delft University of Technology. *Applied Acoustics*, *170*. doi: 10.1016/j.apacoust.2020.107504

Monteiro, F., Merino-Martinez, R., & Lima Pereira, L. T. (2024). Psychoacoustic Evaluation of an Array of Distributed Propellers Under Synchrophasing Operation. In 30^{th} *aiaa/ceas aeroacoustics conference, june 4 – 7 2024, rome, italy.* Retrieved from http://arc.aiaa.org/doi/pdf/10.2514/6.2024-3321 (AIAA paper 2024–3321) doi: 10.2514/6.2024-3321

More, S. R. (2010). *Aircraft Noise Characteristics and Metrics* (Doctoral dissertation, Purdue University). Retrieved from http://web.mit.edu/aeroastro/partner/reports/proj24/noisethesis.pdf (Report No. PARTNER–COE–2011–004)

Osses, A., García León, R., & Kohlrausch, A. (2016). Modelling the sensation of fluctuation strength. In 22^{nd} *international congress on acoustics (ica), september 5 – 9 2016, buenos aires, argentina.* Retrieved from

https://pure.tue.nl/ws/portalfiles/portal/52366479/Osses_Garcia_Kohlrausch_ICA2016_ID113.pdf

Petricelli, F., Chaitanya, P., Palleja-Cabre, S., Meloni, S., Joseph, P. F., Karimian, A., ... Camussi, R. (2023, November). An experimental investigation on the effect of in-flow distortions of propeller noise. *Applied Acoustics*, *214*. doi: 10.1016/j.apacoust.2023.109682

Piccolo, A., Zamponi, R., Avallone, F., & Ragni, D. (2024, June). Towards a Novel Physics-Based Correction to Amiet's Theory for Inflow-Turbulence Noise Prediction. In *30th AIAA/CEAS Aeroacoustics Conference (2024).* Rome, Italy: American Institute of Aeronautics and Astronautics. doi: 10.2514/6.2024-3121

Pockelé, J. S. (2024, April). *Graphical User Interface for the Psychoacoustic Listening Laboratory (PALILA GUI) (version v1.0.0).* Retrieved from https://zenodo.org/doi/10.5281/zenodo.11032101

Quaroni, L. N., Merino-Martinez, R., Monteiro, F. D., & Kumar, S. S. (2024, June). Collective blade pitch angle effect on grid turbulence ingestion noise by an isolated propeller. In *30th AIAA/CEAS Aeroacoustics Conference (2024).* Rome, Italy: American Institute of Aeronautics and Astronautics. doi: 10.2514/6.2024-3209

Ramos-Romero, C., Green, N., Torija, A. J., & Asensio, C. (2023, June). On–field noise measurements and acoustic characterisation of multi–rotor small unmanned aerial systems. *Aerospace Science and Technology*, *141*(108537), 1–17. Retrieved from https://doi.org/10.1016/j.ast.2023.108537 doi: 10.1016/j.ast.2023.108537

Rizzi, S. A., Huff, D. L., Boyd, D. D. J., Bent, P., B., H., Pascioni, K. A., ... Snider, R. (2020). *Urban Air Mobility Noise: Current Practice, Gaps, and Recommendations* (Tech. Rep. No. NASA Technical Memorandum 83199). NASA. Retrieved from https://ntrs.nasa.gov/api/citations/20205007433/downloads/NASA-TP-2020-5007433.pdf

Sabzehee, F., Amiri-Simkooei, A., Iran-Pour, S., Vishwakarma, B. D., & Kerachian, R. (2023). Enhancing spatial resolution of GRACE-derived groundwater storage anomalies in Urmia catchment using machine learning downscaling methods. *Journal of Environmental Management*, *330*, 117180.

Schade, S., Merino-Martinez, R., Ratei, P., Bartels, S., Jaron, R., & Moreau, A. (2024). Initial Study on the Impact of Speed Fluctuations on the Psychoacoustic Characteristics of a Distributed Propulsion System with Ducted Fans. In 30^{th} *aiaa/ceas aeroacoustics conference, june 4 – 7 2024, rome, italy.* Retrieved from http://arc.aiaa.org/doi/pdf/10.2514/6.2024-3273 (AIAA paper 2024–3273) doi: 10.2514/6.2024-3273

Schäffer, B., Pieren, R., Heutschi, K., Wunderli, J. M., & Becker, S. (2021). Drone Noise Emission Characteristics and Noise Effects on Humans - A Systematic Review. *International Journal of Environmental Research and Public Health*, *18*(11), 5940. Retrieved from https://pubmed.ncbi.nlm.nih.gov/34205949/ doi: 10.3390/ijerph18115940

Selig, M. (2003). Low reynolds number airfoil design lecture notes. *VKI Lecture Series, November*, 24–28.

Teunissen, P. J. G. (2000). *Testing theory: an introduction*. Website: http://www.vssd.nl: Delft University Press. (Series on Mathematical Geodesy and Positioning)

Thoma, E. M., Merino-Martinez, R., Grönstedt, T., & Zhao, X. (2024). Noise from Flight Procedure Designed with Statistical Wind: Auralization and Psychoacoustic Evaluation. In 30^{th} *aiaa/ceas aeroacoustics conference, june 4 – 7 2024, rome, italy.* Retrieved from http://arc.aiaa.org/doi/pdf/10.2514/6.2024-3017 (AIAA paper 2024–

3017) doi: 10.2514/6.2024-3017
Tinney, C. E., & Sirohi, J. (2018, July). Multirotor Drone Noise at Static Thrust. *AIAA Journal*, *56*(7), 2816–2826. doi: 10.2514/1.J056827
Torija, A. J., Ramos-Romero, C., & Green, N. (2024). Acoustic and Psychoacoustic Characterisation of Unmanned Aircraft Systems as a Function of Vehicle Mass and Flight Procedure. In 30^{th} *aiaa/ceas aeroacoustics conference, june 4 – 7 2024, rome, italy.* Retrieved from http://arc.aiaa.org/doi/pdf/10.2514/6.2024-3235 (AIAA paper 2024–3235) doi: 10.2514/6.2024-3235
Van Arnhem, N., De Vries, R., Sinnige, T., Vos, R., Eitelberg, G., & Veldhuis, L. L. M. (2020, December). Engineering Method to Estimate the Blade Loading of Propellers in Nonuniform Flow. *AIAA Journal*, *58*(12), 5332–5346. Retrieved 2023-09-19, from https://arc.aiaa.org/doi/10.2514/1.J059485 doi: 10.2514/1.J059485
von Bismark, G. (1974). Sharpness as an attribute of the timbre of steady sounds. *Acta Acustica united with Acustica*, *30*(3), 159–172. Retrieved from https://www.semanticscholar.org/paper/Sharpness-as-an-attribute-of-the-timbre-of-steady-Bismarck/9576a2a74bff46ee0cded25bfd9e4302b4fb0470
Vorländer, M. (2008). *Auralization – Fundamentals of Acoustics, Modelling, Simulation, Algorithms and Acoustic Virtual Reality* (First ed.). Springer. Retrieved from https://www.springer.com/gp/book/9783540488293 (ISBN: 978–3540488293)
Willemsen, A. M., & Rao, M. D. (2010). Characterization of sound quality of impulsive sounds using loudness based metric. In 20^{th} *international congress on acoustics, august 23 – 27 2010, sydney, australia.* Retrieved from https://www.acoustics.asn.au/conference_proceedings/ICA2010/cdrom-ICA2010/papers/p586.pdf
Yunus, F. (2023). *Methodologies and algorithms for sound propagation in complex environments with application to urban air mobility: A ray acoustics approach* (PhD thesis). Delft University of Technology, Delft, The Netherlands.
Yunus, F., Casalino, D., Avallone, F., & Ragni, D. (2023a). Efficient prediction of airborne noise propagation in a non-turbulent urban environment using gaussian beam tracing method. *The Journal of the Acoustical Society of America*, *153*(4), 2362–2362.
Yunus, F., Casalino, D., Avallone, F., & Ragni, D. (2023b). Efficient prediction of urban air mobility noise in a vertiport environment. *Aerospace Science and Technology*, *139*, 108410.
Yunus, F., Casalino, D., Romani, G., & Snellen, M. (2024). Efficient prediction of propller noise at incidence. In *Quite drones symposium (2024).* Manchester, UK.
Yunus, F., Varriale, C., & Snellen, M. (2024). Efficient noise footprint computation for urban air mobility maneuvers in vertiport environments. In *30th aiaa/ceas aeroacoustics conference (2024)* (p. 3335).
Yunus, F., von den Hoff, B., & Snellen, M. (2024). Predicting tonal noise of full-electric propeller-driven aircraft in outdoor environments using low-order models. In *30th aiaa/ceas aeroacoustics conference (2024)* (p. 3418).
Yupa-Villanueva, R. M., Merino-Martinez, R., Altena, A., & Snellen, M. (2024). Psychoacoustic Characterization of Multirotor Drones in Realistic Flyover Maneuvers. In 30^{th} *aiaa/ceas aeroacoustics conference, june 4 – 7 2024, rome, italy.* Retrieved from http://arc.aiaa.org/doi/pdf/10.2514/6.2024-3015 (AIAA paper 2024–3015) doi: 10.2514/6.2024-3015
Yupa-Villanueva, R. M., Merino-Martinez, R., Andino Cappagli, C. I., Altena, A., & Snellen, M. (2024). Effect of Unmanned Aerial Vehicle Configurations on the Acoustic and Psychoacoustic Signatures. In 30^{th} *international congress on sound and vibration (icsv), july 8 – 11 2024, amsterdam, the netherlands.*

Zarri, A., Dell'Erba, E., Munters, W., & Schram, C. (2022). Aeroacoustic installation effects in multi-rotorcraft: Numerical investigations of a small-size drone model. *Aerospace Science and Technology*, *128*, 107762.